Incised valleys on the Algarve inner shelf, northern Gulf of Cadiz margin: Stratigraphic architecture and controlling factors in a low fluvial supply setting

Álvaro Carrión-Torrente [a,b], Francisco José Lobo [a,*], Ángel Puga-Bernabéu [b], María Luján [c], Isabel Mendes [d], Till J.J. Hanebuth [e], Susana Lebreiro [f], Marga García [g], María Isabel Reguera [f], Laura Antón [f], David Van Rooij [h], Javier Cerrillo-Escoriza [a,b]

[a] *Department of Marine Geosciences, Instituto Andaluz de Ciencias de la Tierra—IACT, Spanish Research Council—CSIC and University of Granada—UGR, Avenida de las Palmeras 4, 18100, Armilla, Granada, Spain*
[b] *Departamento de Estratigrafía y Paleontología, University of Granada, Avenida de la Fuente Nueva s/n, 18071, Granada, Spain*
[c] *Department of Earth Sciences, University of Cadiz, Campus Universitario Río San Pedro s/n, 11510, Puerto Real, Spain*
[d] *Centre for Marine and Environmental Research—CIMA, Universidade do Algarve, 8005-139, Faro, Portugal*
[e] *Department of Marine Science, Coastal Carolina University, 301 Allied Drive, Conway, SC, 29528-6054, USA*
[f] *Instituto Geológico y Minero de España-Centro Nacional, Spanish Research Council—CSIC, C/ Ríos Rosas 23, 28003, Madrid, Spain*
[g] *Oceanographic Centre of Cadiz, Spanish Institute of Oceanography—IEO, CSIC, Ministry of Science and Innovation, Muelle de Levante, s/n, Puerto Pesquero, Cádiz, 11006, Spain*
[h] *Renard Centre of Marine Geology, Ghent University, Krijgslaan 281 (S8), 9000, Gent, Belgium*

ARTICLE INFO

ABSTRACT

A network of cross-shelf paleovalleys has been recognized over the paleo-inner shelf off the Gilão-Almargem Estuary, a small fluvial drainage system that presently receives minor sediment supply in the eastern Algarve shelf, northern margin of the Gulf of Cadiz (SW Iberian Peninsula). This study is aimed at determining the driving controls that triggered substantially different paleohydrological conditions and sedimentary dynamics of ancient fluvial systems in this margin. We focus on evidences of secondary controls on valley genesis and evolution, superimposed to primary glacio-eustatic control such as antecedent geology, low fluvial supply and changing hydrodynamic regimes. The architecture and spatial distribution of these paleovalleys were interpreted based on a grid of seismic profiles with different resolutions. Likewise, a sediment core obtained in a distal position of the paleovalley system provided information about sedimentary processes during the most recent stage of valley infilling. The chronostratigraphic framework was constructed based on regional seismic horizons defined in previous studies and complemented with two AMS 14C dates obtained from bivalve shells.

The inner shelf paleovalley system is composed of several incised valley features which exhibit a remarkable similar internal architecture. These inner valley features exhibit two major incision phases (from oldest to youngest; IP 2 and IP 1) that are thought to constitute a simple paleovalley system formed during the last glacial cycle. The origins of the incision are considered to be different. The older one is related to fluvial incision during the sea-level fall leading into the Last Glacial Maximum, whereas the recent one is interpreted as the result of tidal scour during the postglacial transgression. Their corresponding infillings are interpreted, respectively, as estuarine bay-fill deposits and estuary-mouth sands. Overlying the paleovalley infilling, a distinctive reflective unit is in agreement with the generation of coastal barriers and related depositional systems.

The formation of the paleo-inner-shelf paleovalley system was strongly conditioned by antecedent geology, which strongly limited the generation of wide incised valleys and determined the amount of incision landward of a well-defined break of slope. Its postglacial infilling was mainly estuarine in nature, likely involving the

development of a dendritic system, with numerous barriers interrupted by tidal inlets and channels in a mixed estuarine system with low fluvial supply.

1. Introduction

Incised valleys are common stratigraphic features in continental margins, whose development and stratigraphic organization are primarily driven by allocyclic processes such as the rate and magnitude of relative sea-level variations (Dalrymple et al., 1994; Chaumillon et al., 2010; Wang et al., 2020). Other controlling factors include variations of downstream forcing mechanisms such as river and shelf gradients, pre-existent tectonic features and the morphology and nature of antecedent geology, which may offer different resistance to erosion, eventually dictating hydrodynamic processes and sediment supply (Zaitlin et al., 1994; Dalrymple, 2006; Chaumillon et al., 2010). More recent studies highlight the potential genetic role played by upstream controls such as river and sediment discharges (Mattheus and Rodriguez, 2011; Wang et al., 2019), which are ultimately driven by climatic processes (Boyd et al., 2006). Specifically, drainage basin size and climate are correlated with the shape and size of incised valleys (Wang et al., 2019). Ultimately, valley shape exerts a major control on valley-fill preservation (Ashley and Sheridan, 1994).

The nature of valley infilling is mostly determined by the rates of sediment supply and hydrodynamic variables such as waves and tides (Dalrymple et al., 1994; Chaumillon et al., 2010). The balance between hydrodynamics and sediment supply exerts a major control on systems tract preservation (Boyd et al., 2006) and on the formation of distinctive surfaces within incised-valley infillings, such as ravinement surfaces (Zaitlin et al., 1994; Tessier, 2012). Specifically, tidal ravinement surfaces may constitute the most important stratigraphic features locally developing tidal inlets (Ronchi et al., 2018), and extending through the estuarine phase of incised valleys (Tessier, 2012).

There is considerable variability concerning both the stratigraphic architecture and the spatial distribution of incised valleys. With regard to their stratigraphic expression, their complexity varies according to valley size, increasing from small to large drowned valleys (Ashley and Sheridan, 1994). Thus, small valleys tend to be composed of simple sequences, and their architecture is more influenced by the effects of background geology on marine processes (Chaumillon and Weber, 2006; Chaumillon et al., 2008; Menier et al., 2010; Klotsko et al., 2021; De Falco et al., 2022) rather than by the characteristics of catchment areas (Maselli and Trincardi, 2013). As valley size increases, the thickness of fluvial and estuarine deposits increases (Wang et al., 2020) and compound incised valleys may be preserved (Zaitlin et al., 1994), reflecting the influence of superimposed sea-level cycles (Dalrymple et al., 1994).

Considering the spatial variability of incised valleys, most cross-shelf valleys become less distinctive towards the mid to outer shelf, as backwater effects evolve during relative sea-level falls (Blum et al., 2013). As a consequence, valley incision tapers at variable distances from landward coastlines at maximum water depths of 70–80 m (Lericolais et al., 2001; Maselli and Trincardi, 2013). However, in certain outer margin settings, infilled incised valleys with incisions of tens of meters and without a clear connection with inland drainages have been documented (Reynaud et al., 1999; Lericolais et al., 2003; Paquet et al., 2010); the formation of those distal features has been explained as a combined effect of glacio-eustatic cycles and tectonic processes, such as tilting or local tectonic uplift (Reynaud et al., 1999; Burger et al., 2001).

The northern Gulf of Cadiz margin is mainly supplied by two major rivers (Guadiana and Guadalquivir) whose continued sediment flux has driven the outward margin growth at least during the late Quaternary (Hernández-Molina et al., 2000; Lobo et al., 2005; Mestdagh et al., 2019). Of these major rivers, recent investigations have mapped incised valley features off the Guadiana River (Lobo et al., 2018). West of the Guadiana River, the Algarve coast in southern Portugal is dominated by

an extensive barrier-lagoon system (i.e., the Ria Formosa system) with reduced fluvial supply. However, at the eastern tip of the barrier system, a small drainage basin comprising the Gilão and Almargem rivers is developed. The fluvial outlet is partially protected by the coastal barrier; therefore, fluvial flux towards the adjacent shelf should be regarded as negligible. Nevertheless, preliminary inspection of available seismic records of the fluvial outlet of Gilão and Almargem rivers reveals the occurrence of abundant incised valley features; this observation is counterintuitive with the low importance of adjacent river basins, likely suggesting the existence of significant hydrological changes during the recent past.

Bearing in mind these preliminary observations, the present study aims at characterizing a network of incised valleys in the inner shelf of the eastern Algarve shelf, framing them in the chronostratigraphic scenario available for the northern Gulf of Cadiz shelf and discussing the driving factors which may have enabled the formation and/or eventual preservation of incised valleys in a presently under-supplied shelf.

2. Regional setting

This study focuses on paleovalley systems off the eastern Algarve coast (Portugal), offshore the Gilão-Almargem Estuary (Fig. 1a). The eastern Algarve coastline is located in the passive continental margin of the Gulf of Cadiz (southwestern Iberian Peninsula) between the Ria Formosa barrier system to the west and the Guadiana River estuarine system to the east (Fig. 1a).

2.1. Geological setting

The Algarve Basin extends from inshore, where a Paleozoic basement and a flysch sequence of slates and greywackes crop out, to offshore where the basin fill is composed of Mesozoic and Cenozoic sedimentary rocks (Terrinha, 1998). A passive extensional margin with continental siliciclastics and marine carbonates was developed in the Mesozoic. The margin evolved towards the early Miocene to a terrigenous regime under active transcurrent tectonics near the Iberian-African plate boundary (Maldonado and Nelson, 1999; Ramos et al., 2016). The Cenozoic evolution of the Algarve Basin was determined by the reactivation of N–S to NW-SE Hercynian basement structures and by halokinesis of a thick evaporitic unit (Lopes et al., 2006; Vázquez et al., 2010; Ramos et al., 2016).

The early Pliocene witnessed the instauration of a terrigenous drift regime (Maldonado and Nelson, 1999). The late Pliocene-Quaternary was dominated by glacio-eustatic sequences mainly composed of regressive and lowstand deposits (Hernández-Molina et al., 2002); 100 ka sequences have been formed after the Mid Pleistocene Transition (MPT) in response to a significant increase in sea-level amplitudes (Maldonado and Nelson, 1999; Hernández-Molina et al., 2002; Mestdagh et al., 2019). A number of deformational features on the eastern Algarve Shelf indicate neotectonic activity predating and postdating the MPT (Mestdagh et al., 2019; Luján et al., 2020).

2.2. Coastal configuration

The eastern Algarve shelf is located between two major coastal features: the Ria Formosa Barrier Island System (RFBIS) to the west and the Guadiana River estuary to the east (Fig. 1a). The RFBIS is composed of five barrier islands and two peninsulas that enclose a coastal lagoon (Fig. 1a) which covers an area of 8.4×107 m^2 with an average water depth of 2 m (Andrade, 1990). The islands and peninsulas are separated by six tidal inlets that protect the lagoon from the direct impact of

marine waves (Fig. 1a). The barrier islands are actively changing due to tidal inlet dynamics (Vila-Concejo et al., 2006; Pacheco et al., 2010) and to longshore drift (Ciavola et al., 1997; Garcia et al., 2002), characterizing a highly dynamic system.

The Holocene evolution of the RFBIS implies three main steps (Pilkey et al., 1989; Sousa et al., 2014, 2019): (1) marine flooding of paleovalleys in the early Holocene; (2) development of a proto-barrier during the early-middle Holocene; (3) full development of the barrier and enclosing of the coastal lagoon from the middle Holocene to the present.

The Gilão-Almargem Estuary forms in front of Tavira, protected by Tavira and Cabanas barriers which are separated by the Tavira inlet (Fig. 1b). The inner part of the estuary contains an almost continuous record of sediment accumulation in a tidal flat/salt marsh environment. However, the outer barriers are the result of more discontinuous processes (Boski et al., 2008). Indeed, the present barrier was formed in the sixteenth century (Veiga-Pires et al., 2000). Until then, the Gilão-Almargen estuary was open to the ocean (Rocha et al., 2004).

In the vicinity of the study area, the major sediment source is provided by the fluvial input from the Guadiana River (Fig. 1a), which drains most of the southern half of the Iberian Peninsula with a catchment area of about 67,000 km^2 (Boski et al., 2008; Lobo et al., 2018).

The hydrologic regime of the Guadiana River is characterized by large intra- and intra-annual discharge variability, with mean annual discharges of 80–160 m^3 s^{-1} (van Geen et al., 1997) and inter-annual discharge variability between extremely low levels in summer and maximum levels during winter (up to 11,000 m^3 s^{-1}) (Rocha and Correia, 1995).

2.3. The eastern Algarve shelf

The Algarve Shelf shows a narrow and steep morphology. Shelf width increases from 5 km in the south-western area, off the city of Faro, to 25 km off the Guadiana River mouth (Lobo et al., 2001; Hernández-Molina et al., 2006). The shelf break occurs between 140 and 150 m water depths (Fig. 1; Baldy, 1977; Vanney and Mougenot, 1981). Three shelf domains have been distinguished in the Gulf of Cadiz northern margin according to the nature of surficial sediments (Fig. 1b; Nelson et al., 1999, Lobo et al., 2000, 2018; Maldonado et al., 2003, Gonzalez et al., 2004). The proximal domain is located on the inner shelf, down to 30 m water depth, and is covered by sandy deposits and scattered rocky outcrops which show a parallel-to-shoreline distribution (Fig. 1b; Rey and Medialdea, 1989; Fernández-Salas et al., 1999). The middle domain
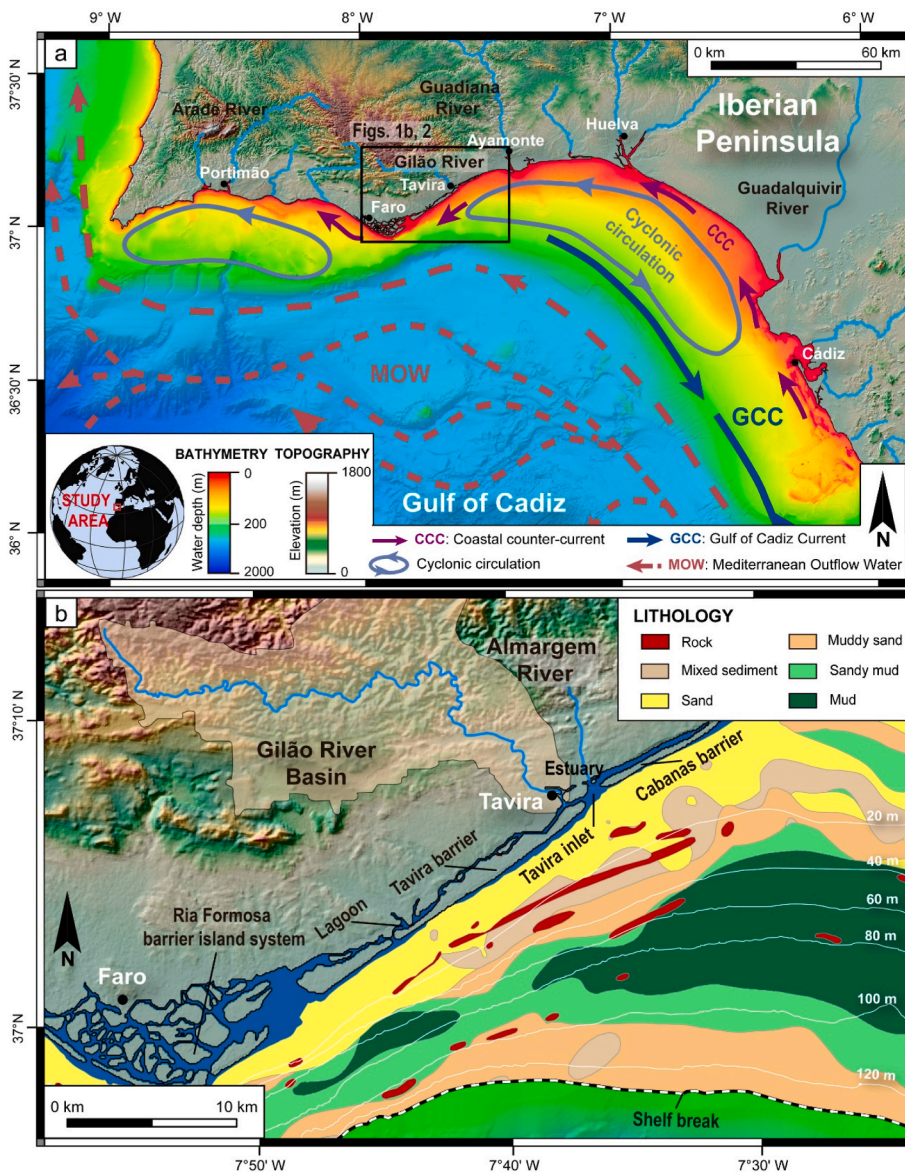

Fig. 1. a) Topo-bathymetric map showing the location of the study area (inset) on the eastern Algarve shelf (Portugal), offshore the Gilão-Almargem Estuary, in the northern Gulf of Cadiz. The main rivers and pathways of the main water masses and currents are also indicated. Topography from Spanish National Geographic Institute, 2015) (MTN50 raster). Bathymetry from EMODnet Bathymetry Consortium, 2020. b) Map showing the sediment distribution on the shelf in the study area offshore of the Guadiana River mouth (extracted from Gonzalez et al., 2004) and the Gilão River basin.

is located between 30 and 100 m water depths, and it is characterized by muddy sediments composed of muds and sandy muds (Fig. 1b; Gonzalez et al., 2004). The distal domain is located on the outer shelf deeper than 100 m water depths and mainly exhibits muddy sands (Fig. 1b; Nelson et al., 1999; Gonzalez et al., 2004).

The eastern Algarve shelf receives at present minor fluvial or marine sediment supplies. Small rivers such as the Gilão and Almargem with a total catchment of ca 290 km^2 drain Mesozoic carbonatic and Miocene siliciclastic substrates. The average precipitation in this region for the last 75 years is 530 mm yr^{-1} and is concentrated between October and April. The inner shelf sediment distribution exhibits significant along-shore variability, due to the major influence of coastal processes, such as littoral drift and storm currents (Bosnic et al., 2017). However, this region receives a low amount of sand, as these sediments tend to be trapped in inlets located to the west (Rosa et al., 2013).

2.4. Oceanographic regime

In the Gilão-Almargem Estuary area, the longshore current is west-to-east and the tidal regime is mesotidal and semi-diurnal with a mean range of 2.20 m (Boski et al., 2008). The wave regime is predominantly from the southwest, associated mainly with moderate-energy Atlantic swells. Storm events are frequent in autumn and winter, generating significant wave heights of 4–7 m (Del Río et al., 2012; Plomaritis et al., 2015). Measurements of the depth of closure in the Algarve coast provide values of up to 10 m water depth during high-energy periods (Dolbeth et al., 2007).

The surface circulation between the RFBIS and the Guadalquivir River is characterized by a cyclonic pattern (García-Lafuente et al., 2006). Inner shelf waters (<30 m water depth) are periodically affected by poleward coastal counter-currents (Garel et al., 2016). The outer shelf is swept by the Gulf of Cadiz Current (GCC), a branch of the Portuguese-Canary eastern boundary current that transports Eastern North Atlantic Central Waters towards the Strait of Gibraltar (Fig. 1a; Bellanco and Sánchez-Leal, 2016).

3. Material and methods

The present study is based on a combined seismic stratigraphic and sedimentological analysis, focusing on evidences of incised valleys in the eastern Algarve shelf. The chronostratigraphic framework was constructed based on two radiocarbon (^{14}C) accelerated mass spectrometry (AMS) ages and in regional seismic horizons defined in previous studies (Mestdagh et al., 2019; Luján et al., 2020). Additionally, the bathymetric information used in this study was compiled from the European Marine Observation and Data Network Bathymetry portal (EMODnet, 2020) with a horizontal resolution of 115 m.

3.1. Material

3.1.1. Seismic profiling

This study is based on the interpretation of different types of seismic data collected on the continental shelf between Faro (Portugal) and the Guadiana River mouth. The main dataset used for the seismic interpretation is composed of high-resolution seismic reflection profiles acquired during two oceanographic surveys in 2013: COMIC onboard *RV Belgica* and LASEA 2013 onboard *RV Ramón Margalef*. Two types of seismic data were acquired: parametric echo sounder acoustic profiles (TOPAS) and sparker single-channel seismic profiles. Additionally, the aforementioned data are complemented with seismic data from previous surveys in the study area, such as the GOLCA 93, FADO 96 and WADI-ANA 2000 surveys, which used a Uniboom source (Geopulse™) (Fig. 2).

The grid of TOPAS sub-bottom seismic data was acquired during the LASEA 2013 survey and summed a total length of 1450 km across- and along-shelf profiles from 20 m water depth to around the shelf break (Fig. 2). TOPAS acquisition was achieved by a chirp (LFM) pulse form with transmitting frequencies of 1.5–5.5 kHz, a pulse length of 5 ms, and a power level of −2 dB. The sample rate was 30 kHz and the trace length was 200 ms. Post-processing included reflection strengthening, delay corrections, first break picking, time variable gain, spike removals, tide and swell static corrections, and top muting.

Seismic profiles acquired with a SIG sparker source were collected during the LASEA 2013; COMIC 2013 surveys and provided higher penetration. Sparker profiles were collected for approximately 700 km generally following or paralleling the track of the TOPAS profiles (Fig. 2). Acquisition was made with a 300 J seismic source, a vertical resolution of about 1.5 m, and a 75 m long SIG single-channel streamer; the shot interval was 2 s, the sampling frequency was 10 kHz and the trace length varied between 0.5 and 2 s. Post-processing included correction of navigation offset, gains, bandpass filtering, demultiple,
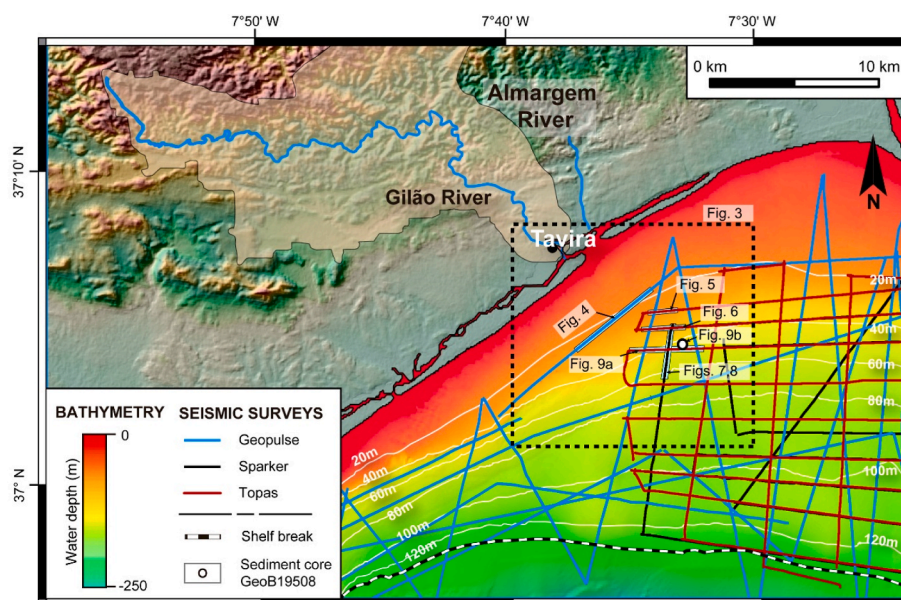

Fig. 2. Location of the seismic database on the shelf in the study area offshore of the Gilão-Almargem Estuary (EMODnet Bathymetry Consortium, 2020). The location of Fig. 3 is indicated in the inset rectangle, and the location of Figs. 4–9 is highlighted.

tidal and swell static corrections, and top muting.

Uniboom source profiles (Fig. 2) have a cumulative total length of more than 1500 km. The approximate vertical resolution of the system is 1–1.5 m. Basic post-processing included bandpass filtering, amplitude corrections (spherical divergence), 2D spike removal (burst noise removal), swell static corrections and top muting.

Vertical scales of the different seismic profiles are expressed here in milliseconds for two-way travel time (TWTT), which was converted to meters below the present sea level (mbpsl) using a mean velocity of 1500 m s^{-1}.

3.1.2. Sediment core data

A sediment core (GeoB19508) obtained during the CADISED 2015 oceanographic survey onboard *RV Poseidon* was also studied to characterize the distal termination of an incised valley (Fig. 2). The sediment core has a total length of 494 cm and was collected using a vibrocorer device.

The lithological description of the sediment core was carried out through the observation of high-resolution digital images. In addition, grain size analyzes were performed on sixteen samples collected along the sediment core at intervals ranging from 20 to 35 cm, enabling the determination of statistical parameters (mean, sorting, skewness and kurtosis). Hydrogen peroxide was used to eliminate the organic matter. Fine and coarse fractions were wet separated using a 63 μm (4 phi) sieve. The grain size distribution of the fine fraction was analyzed with the pipette method and the coarse fraction was subdivided by dry sieving using a sieve rack. Both fractions were graded in phi intervals. Grain size parameters were obtained using the Geometric Method of Moments and the textural classification after Folk (1954). In parallel to this analysis, a carbonate-content analysis (calcimetry) was carried out in two grain size classes (medium sand and gravel). At least 2 g per sample were treated with HCl (0.1M) for carbonate dissolution and subsequently, the samples were put in standby for 24 h prior to being centrifuged.

3.1.3. Radiocarbon dating

Two AMS ^{14}C dates were obtained from mollusk shells without signs of transport or diagenetic alteration (Table 1). Dating was carried out at CNA-Centro Nacional de Aceleradores (Sevilla, Spain). Age calibration was performed with the Calib 8.2 software (Stuiver et al., 2021), using conventional radiocarbon ages and the MARINE 20 calibration data set (Heaton et al., 2020) and in which the local reservoir effect (ΔR) was not applied. The median of the probability distribution was used as a reliable estimation of the sample's calendar age (Telford et al., 2004). For years given with the notation BP (Before Present), the zero age is 1950 CE. Gregorian calendar years (BCE/CE) were considered for historic ages.

3.2. Interpretation procedure

3.2.1. Seismic interpretation

Seismic horizons and discontinuities were interpreted following a standard seismic stratigraphy procedure (Mitchum, 1977), enabling the definition of seismic units using the commercially available software IHS Kingdom™. These data were subsequently exported and mapped using ArcGIS™ software. We attempted the interpretation of incised valley systems based on current knowledge of incised valleys seismostratigraphic patterns, architectures, and bounding surfaces. (e.g., Vail, 1987; Boyd et al., 2006; Catuneanu et al., 2011; Gomes et al., 2016; Aquino da Silva et al., 2016). The depositional sequence boundary for each incision phase marks the basal reflection and it is associated with valley incision during relative sea-level falls. Transgressive surfaces (TS; Posamentier and Vail, 1988) are related to the flooding of the valleys and subsequent infilling (Vail 1987; Catuneanu et al., 2011). Valley infillings exhibit typical seismostratigraphic patterns, such as onlap and downlap terminations, vertical accretions, and truncated surfaces (e.g., Aquino da Silva et al., 2016; Gomes et al., 2016).

Age attribution of the seismic horizons (Fig. 3) was made through the correlation of the regional seismic grid with sites U1386 and U1387, drilled during IODP expedition 339 (Hernández-Molina et al., 2016; Mestdagh et al., 2019; Luján et al., 2020). This correlation was based in the seismic stratigraphic framework for the northern Gulf of Cadiz continental margin, carried out by Mestdagh et al. (2019), where two seismic profiles on middle slope were connected to the seismic grid on the upper slope and the shelf, allowing to illustrate the lateral variability in the seismic stratigraphic architecture both downslope (shelf vs. upper slope vs. middle slope) and along-strike. Afterwards, the major regional seismic surfaces were continued westward across the shelf around the Guadiana River by Luján et al. (2020), allowing us to constraining the relative ages of the incised valleys by using these major regional seismic surfaces.

3.2.2. Sedimentological interpretation

Descriptions of the lithology, grain size texture, sedimentary structures, bioturbation, and carbonate content analysis from core GeoB19508 (Fig. 2) were used in order to obtain information on the sedimentary processes during the most recent stage of paleovalley sediment infilling.

4. Results

4.1. Seismic stratigraphy of the inner-shelf paleovalley system

Along the inner shelf off the Gilão-Almargem Estuary, a paleovalley system was identified between 10 and 40 m water depths (Fig. 3). The paleovalleys are carved in a well-marked unconformity, which has been correlated with a major regional seismic surface defined across the northern Gulf of Cadiz shelf in previous studies (Luján et al., 2020; Mestdagh et al., 2019). The unconformity is characterized by low proximal gradients (0.29°–0.4°) and a distal break of slope at about 30–40 m water depth that runs at around 6–7 km from the coastline (Fig. 3). In the intervalley areas of the inner shelf, the unconformity is eroding laterally extensive, highly reflective deposits, showing frequent

Table 1
AMS radiocarbon data obtained on shells in the studied sediment cores.

Core ID	Core section	Depth in core (cm)	Sample code	Sample material	δ13C ‰	pMC	Conventional Age ^{14}C BP	cal yr BP (68.3%-1s)	cal yr BP (95.4%-2s)	Median probability[a]	Relative area under probability distribution 1.000 [b]
GeoB19508	IV	274	GeoB08-274	Mollusk shells	0.14 ± 1.5	31.57 ± 0.14	9261 ± 36	9968–9735	10100–9659	9880	1
GeoB19508	IV	329	GeoB19508-329	Mollusk shells	3.46 ± 1.5	30.51 ± 0.15	9535 ± 39	10310–10149	10427–10069	10248	1

[a] Online program Calib.8.2, which uses the marine20.14c calibration dataset recommended for marine samples limited to 603-50,788 14C year BP (Stuiver et al., 2021; Heaton et al., 2020).
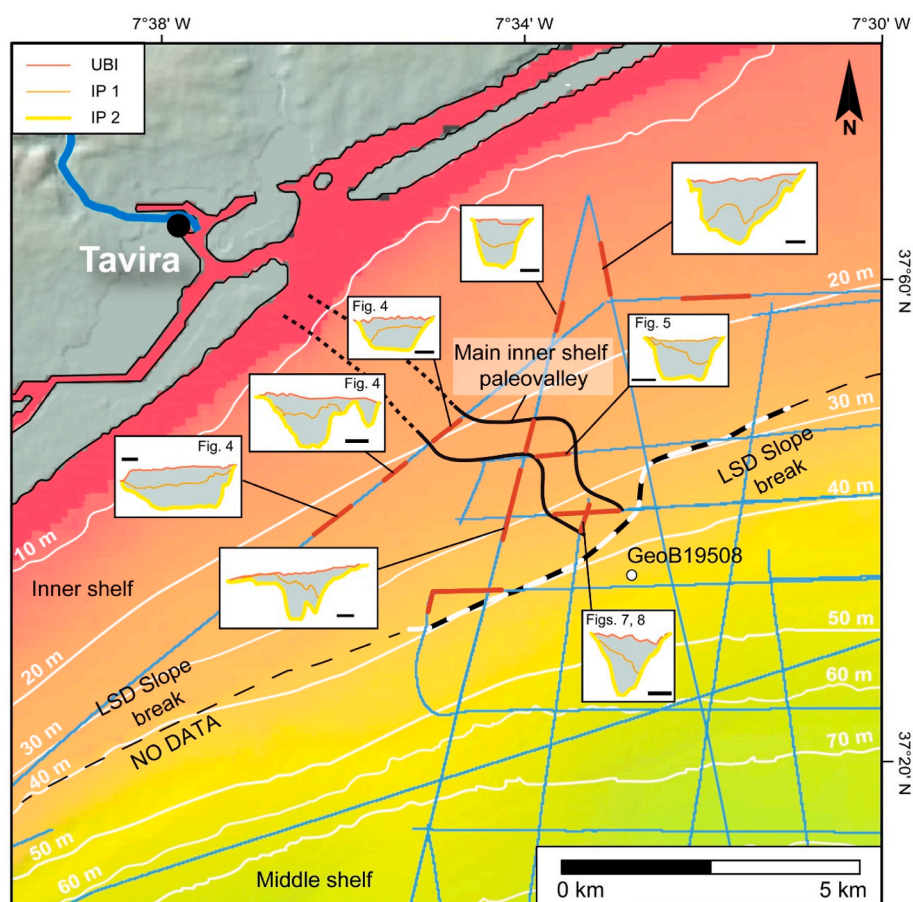[b] Heaton et al., (2020).

Fig. 3. Spatial distribution and schematic cross-sections of the different incised valley features identified along the Algarve inner shelf off the Gilão-Almargem Estuary. The trace of the main fluvial valley which can be considered the seaward extension of the Gilão River is also represented. Background information consists of shelf bathymetry, the Last Subaereal Discontinuity (LSD) slope break line, and the position of sub-bottom seismic lines. UBI: Upper boundary of infilling; IPs 1 and 2: Incised phases 1 and 2.

erosional truncations (Fig. 4). Seaward of the break of slope, gradients of the unconformity increase to values of 0.79°–1.07°.

The inner-shelf paleovalley system is composed of several incised features that could be identified along the available seismic sections (Figs. 4 to 9a). These valleys which constitute the inner-shelf system have small widths and incision depths, with maximum values, respectively, of 650 m and around 30 m below the seafloor (mbsf; Figs. 4–8). Evidences of tectonic activity are not found in this area. The inner-shelf paleovalley system is composed of a main valley that can be followed along 8 km in a NW-SE trend from the present coastline, off the Gilão River mouth (Fig. 3). This main valley could be traced incising the shelf from depths of 20–30 mbsf. This valley has a mean width of 250 m and a mean maximum incision depth of 15 mbsf along the thalweg. Besides, smaller valleys (150–200 m of width) are located at both sides of the main valley. The continuity of these lateral valleys on the shelf was difficult to capture due to the sparse seismic coverage in this area.

Seaward of the break of slope that establishes the boundary of the inner shelf, other valley features are observed (Fig. 7). However, they occur at considerably higher depths (80–100 mbpsl) than the inner shelf valleys, they are less abundant and exhibit blocky seismic facies with some hyperbola, which could indicate older ages. Because of those reasons, we suspect that these distal valleys may be not genetically linked with the inner shelf valleys, and therefore these features are beyond the scope of this study.

The different inner-shelf incised valleys exhibit a similar stratigraphic architecture, where two incision phases (IPs 2 and 1) and their subsequent infillings (ISUs 2 and 1) could be characterized. The incised valleys and their infillings are buried by a reflective sheet-shaped seismic unit, which in turn is overlain a rather transparent surficial seismic unit (Table 2; Figs. 4–8).

The oldest incision phase (IP 2) has incision depths that range from 15 mbsf in proximal areas (Fig. 4) until 32 mbsf in the more distal southeastward parts of the paleovalleys. It is characterized by an erosional high-amplitude seismic horizon which truncates the underlying reflective shelf seismic facies. Generally, these channels show nearly symmetrical U-shaped cross-sections characterized by a central thalweg (Figs. 4–8).

The infilling of the oldest incision phase has a variable spectrum (ISU2; Table 2). It is generally characterized by a moderate to low continuity, sub-parallel seismic configuration (Figs. 4–8). However, a higher level of complexity is identified locally, where ISU 2 is constituted by several sub-units with mostly chaotic, highly reflective seismic configurations bounded by rather irregular horizons, intercalated between sub-parallel configurations (Fig. 5).

The younger incision phase (IP 1) of the inner paleovalley system is characterized by a high-amplitude seismic horizon that truncates the older phase (Figs. 4–8). This phase excavates the shelf from a range of incision depths of 10 mbsf in the proximal areas to around 22 mbsf basinward. During this phase, channels cross-sections display variable geometries that range from symmetric to asymmetric, characterizing both U-shaped and V-shaped cross-sections (Figs. 4 and 7), although asymmetric shapes with laterally displaced valley thalwegs are more common (Figs. 4, 5, 7 and 8).

The infilling of the younger incision phase (ISU 1) is characterized by chaotic, variable amplitude seismic configurations or by non-stratified, massive seismic facies (Table 2; Figs. 4–8); additionally, infilling facies which exhibit lateral migration with some weak tangential-oblique internal reflections are also identified (Fig. 4). The infilling has an average thickness of 9 m, reaching a maximum of 14 m in some valleys.

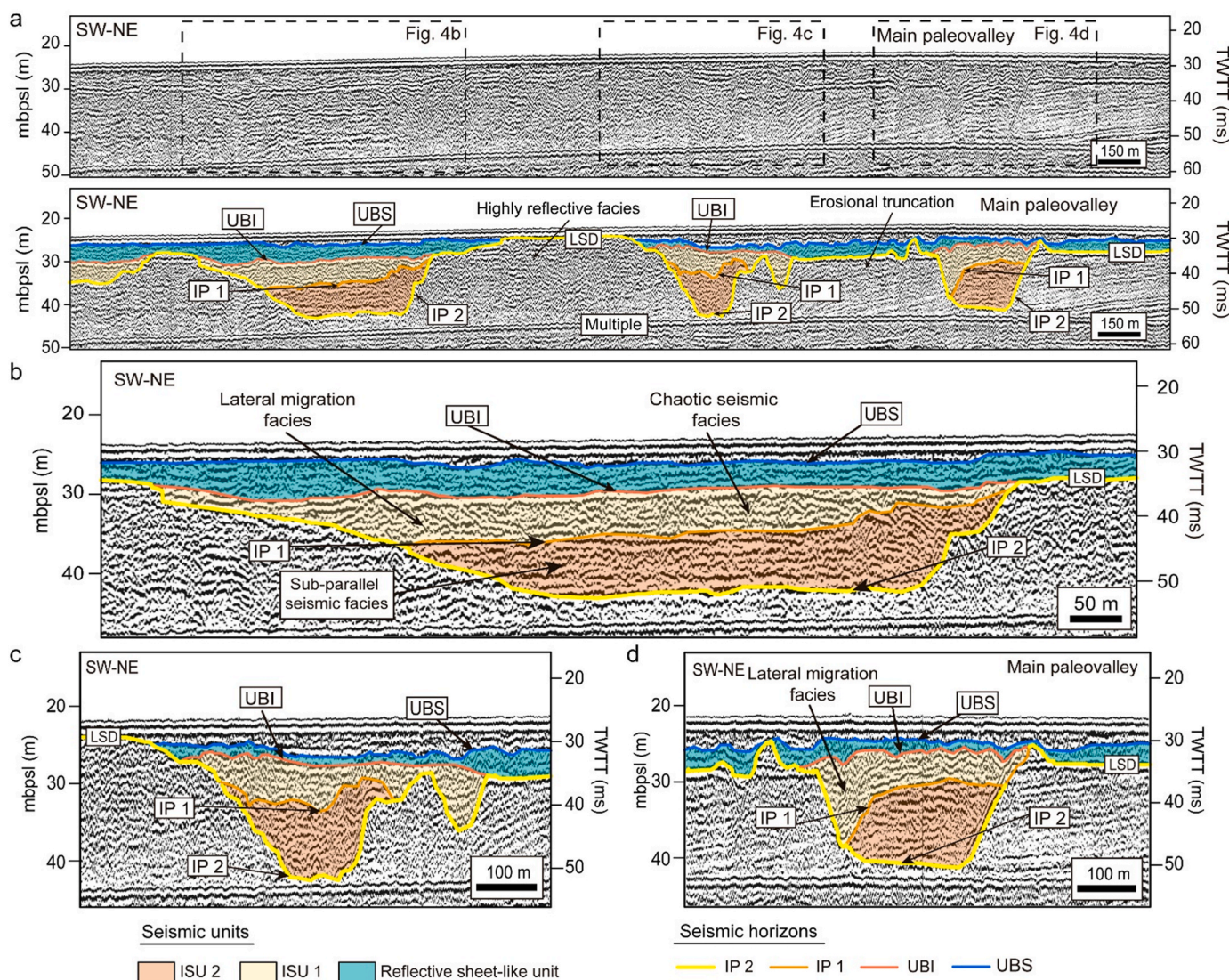The two incision phases are bounded at the top by a high-amplitude,

Fig. 4. a) Coast-parallel (SSW-NNE-oriented) sub-bottom seismic Uniboom source (Geopulse™) profile focusing on the proximal inner-shelf paleovalley system (up) and its interpretation (below). b, c, d) Interpreted zoomed seismic windows of the different paleovalleys. Their location is indicated in Fig. 4a. Here, the important characteristics observed are: the occurrence of highly reflective seismic facies in the intervalley areas with local identifications of well-marked erosional truncations; the distinctive seismic facies which compose the infilling of the paleovalleys, with sub-parallel facies infilling the older incision phase (ISU 2) and with chaotic facies with local occurrences of lateral migrations infilling the younger incision (ISU 1); the asymmetric shape of the younger phase IP 1, with thalwegs displaced laterally; and the thin, laterally extensive reflective unit covering the incisions. The color code and acronyms are indicated here, and the location of the seismic section is indicated in Fig. 2. IPs 1 and 2: Incised phases 1 and 2; UBI: Upper boundary of infilling; UBS: Upper boundary of sheet-like unit.

mostly flat surface which separates the infilling from the upper deposits (Upper boundary of infilling (UBI); Figs. 4–8).

The paleovalley system is buried along the inner shelf by a sheet-like reflective unit that locally exhibits internal reflections, usually sub-parallel but locally also landward dipping (Figs. 4–9); its upper boundary is marked by a mostly flat seismic horizon (UBS). The sheet-like reflective unit buries the paleovalleys and their infillings and extends laterally along intervalley areas beyond the confines of the previous depressions. In proximal areas (20–25 mbpsl), the unit is very thin (i.e., few meters thick), but it thickens in more distal locations, where it might reach 12 m in thickness in areas where the main paleovalley seems to be under filled by previous deposits (Fig. 7). There, at least two tabular deposits seem to be vertically stacked. In more distal locations, the thickness of the sheet-like reflective unit decreases again to values of 5 m, where the reflective unit exhibit mounded features (Fig. 9a). The sheet-shaped reflective unit is covered by a rather transparent drape over most of the inner shelf, increasing the thickness to values of 8–10 m

in distal locations (Figs. 7 to 9a).

4.2. Sedimentary facies and core descriptions

4.2.1. Sedimentary facies

The sedimentological analysis of the available sediment core obtained from the inner-shelf paleovalley system (Figs. 2, 3 and 9a), allow us to distinguish three main sedimentary facies types, which provide useful information about the sedimentary processes during the most recent stage of valley sediment infilling:

Facies Sc: Massive cemented sands. These facies are composed of well-sorted gravelly sands with abundant granule-to pebble-sized bioclasts, mainly bivalves and gastropods. This facies is generally homogenous and massive (Fig. 9b); in addition, strong to slight cementation is observed.

Facies G: Sandy gravels. This facies comprises granule-to pebble-sized gravels, mainly composed of highly fragmented bivalve shells and
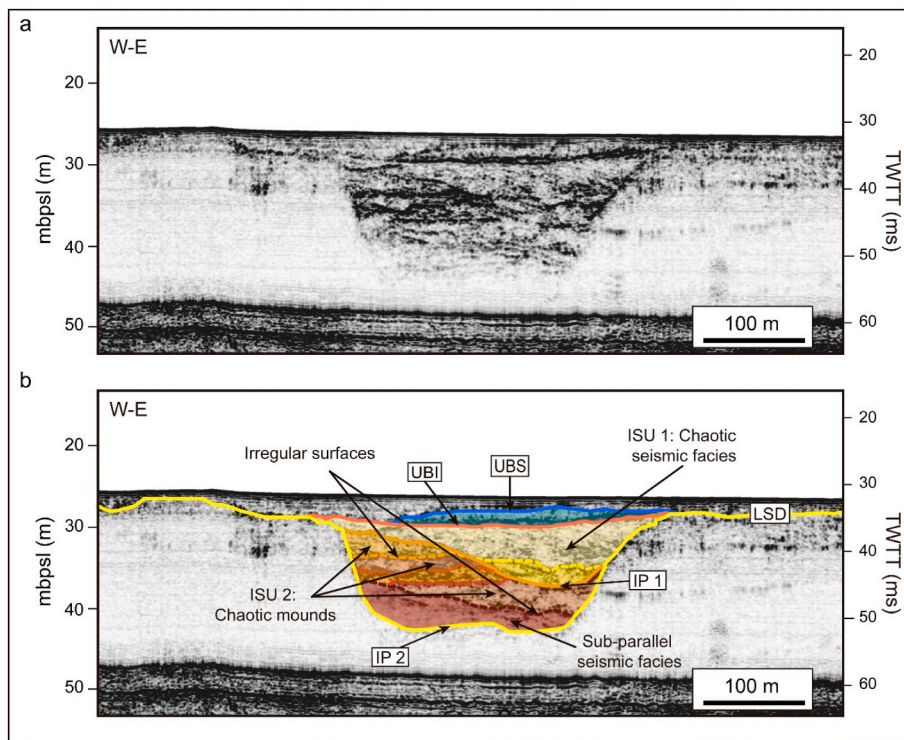
Fig. 5. Along-shelf (W-E-oriented) sub-bottom acoustic profile showing the main inner-shelf paleovalley (a) and its interpretation (b) at around 30 m water depth. The infilling of the lower incision phase (ISU 2) is very complex, with the occurrence of erosional irregular surfaces and chaotic mounds intercalated within sub-parallel seismic facies. The younger incision phase is asymmetrical, with the thalwegs displaced eastward. The infilling of the younger incision phase exhibits a chaotic seismic configuration. The upper reflective unit is not laterally continuous at this location. The location of the seismic section is indicated in Fig. 2 and the color code and acronyms are indicated in Fig. 4.
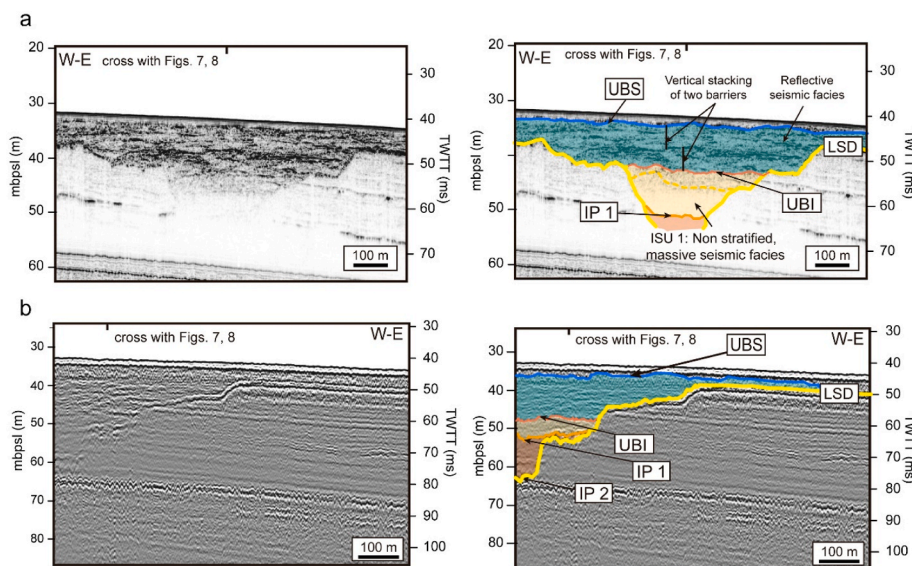

Fig. 6. Along-shelf (W-E-oriented) sub-bottom seismic profiles focusing on the main inner-shelf paleovalley. a) TOPAS acoustic profile (left) and its interpretation (right). b) Sparker profile (left) and its interpretation (right). In the acoustic profile, the lack of penetration prevents the recognition of the oldest incision phase and its infilling. The reflective sheet-shaped unit that covers the paleovalley and its infilling is very thick (10 m) at this location, where an internal high-amplitude reflection separates two sheet-like deposits. The color code and acronyms are indicated in Fig. 4. The location of the seismic section is indicated in Fig. 2. The crossings with Fig. 7 and 8 are also indicated.

rounded rock grains, which are hosted in a mixture of fine to coarse sands and silty sands. This facies is poorly sorted and structureless (Fig. 9b).

Facies Sm: Massive muddy sands. This facies is composed of well-sorted sands without sedimentary structures and with large amounts of bioclasts, mainly bivalves and gastropods. This facies is homogenous and massive (Fig. 9b), although silt nodules of varying sizes are scattered in the sands.

4.2.2. Sediment core GeoB19508

This sediment core is 491 cm long and is composed mainly of sands and gravels (Fig. 9). A correlation between the seismic data and the core projected position was made (Fig. 9a). Such correlation indicates that the core penetrates through the sheet-like reflective unit over the LSD

surface between 50 and 60 mbpsl (Fig. 9a). Nevertheless, at the core location there is not any evidence of any incised feature, and the closer paleovalley is located 3.5 km westward (Fig. 9a).

From bottom to top, four intervals can be distinguished (Fig. 9b). The lower interval (491-436 cm deep; Fig. 9b) is characterized by widely cemented well-sorted sands (facies Sc) with some gravel-sized bioclasts (mollusk and gastropods). The second interval (436-345 cm deep) is dominated by homogenous medium to coarse sands with scarce pebbles (facies Sc). Along this interval, changes in sand cementation are observed: slightly cemented sands occur from 436 to 398 cm that are overlaid by strongly cemented sands from 398 to 381 cm. Then, slightly cemented sandstones occur from 381 to 360 cm. This latter cemented sand interval is interrupted by three mud layers (360-355 cm). Finally, the upper part of this second interval is characterized by highly

cemented sands (355-345 cm). The third interval (345-262 cm deep) is dominated by sandy gravels, although grain sizes increase to around 315 cm deep and decrease in the upper part. The gravel is composed of pebble-sized clasts from a wide variety of lithologies with some shell fragments (facies G). Two AMS ^{14}C dates were obtained in this interval (Table 1), providing age values that place the formation of these deposits between 9880 and 10248 cal yr BP (Fig. 9b). Finally, the upper part of the core (262-0 cm) is characterized by homogeneous fine to medium muddy sands (facies Sm) finning upward. This interval does not show any sedimentary structures and contains some silt nodules of variable size.

Mean grain size shows slight variations along the core ranging from 2.27 to −0.55 phi, with a mean value of 1.43 phi (Fig. 9b). These variations mostly occur in the third interval that has a mean value of −0.14 phi; the rest of the core shows values close to the mean grain size. Sorting values range from moderately well sorted in the top to poorly sorted in some intervals (Fig. 9b). Skewness and kurtosis show similar distributions along the entire core, characterized as coarse skewed and very leptokurtic; the main changes are found in the third interval

(Fig. 9b), which shows a symmetrical skewness and a leptokurtic range.

Calcimetry analyzes reveal high and homogenous carbonate contents in the medium sand fraction, reaching up to 90% along most of the core (Fig. 9b). Meanwhile, the granule fraction shows a lower carbonate content along most of the core, ranging from 10% to 40%; the only exception to this trend occurs in the third core interval, where granule-sized grains have carbonate contents to 90% (Fig. 9b).

5. Discussion

5.1. Regional chronostratigraphic framework

Off the Guadiana River, major shelf erosional unconformities were correlated with the late Quaternary 100 ka glacio-eustatic cycles from 435 to 27 ka (Fig. 10a; Mestdagh et al., 2019). These surfaces were identified in the outer shelf; however, the lateral tracing of these shelf erosional surfaces revealed that they tend to merge landward and westward, generating protracted hiatuses that increase in magnitude in those directions (Luján et al., 2020) (Fig. 10a). Based on the study by
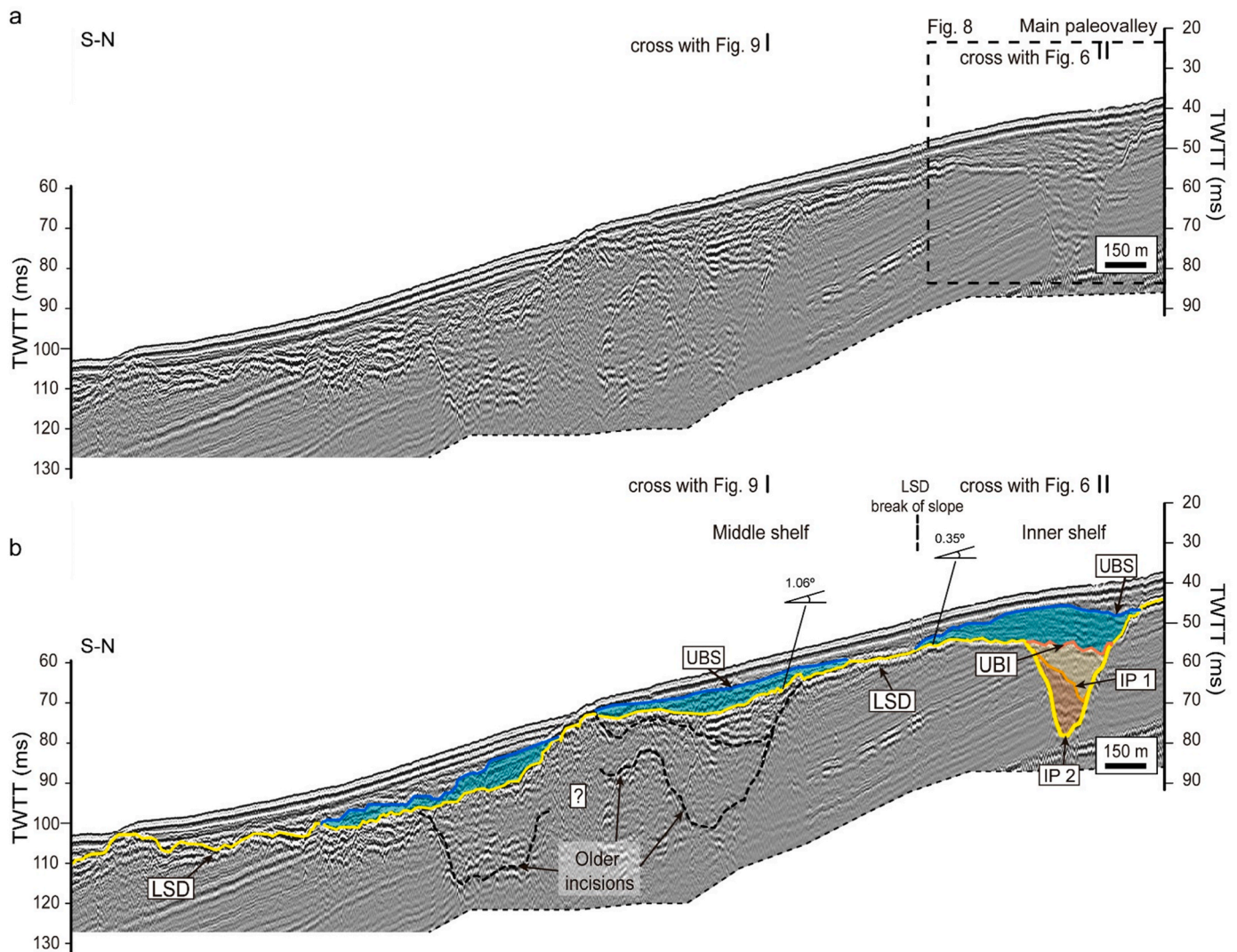

Fig. 7. Downdip cross-shelf (S–N oriented) Sparker profile (a) and interpretation (b) showing the occurrence of valleys landward and seaward of the break of slope that establishes the seaward boundary of the paleo-inner shelf. Landward of the break of slope, the main inner shelf paleovalley is observed at an approximate depth of 40–80 ms (more details of this valley are provided in Fig. 8). Seaward of the break of slope, several valley features occur at water depths of 39 m. Here, the paleovalleys seem to be covered by blocky, highly reflective seismic facies, and the lateral flanks of the valleys are not easily identified. The location of the seismic section is indicated in Fig. 2 and the color code and acronyms are indicated in Fig. 4. The location of Fig. 8 (inset rectangle), and the crossings with Fig. 6 and 9 are also indicated.
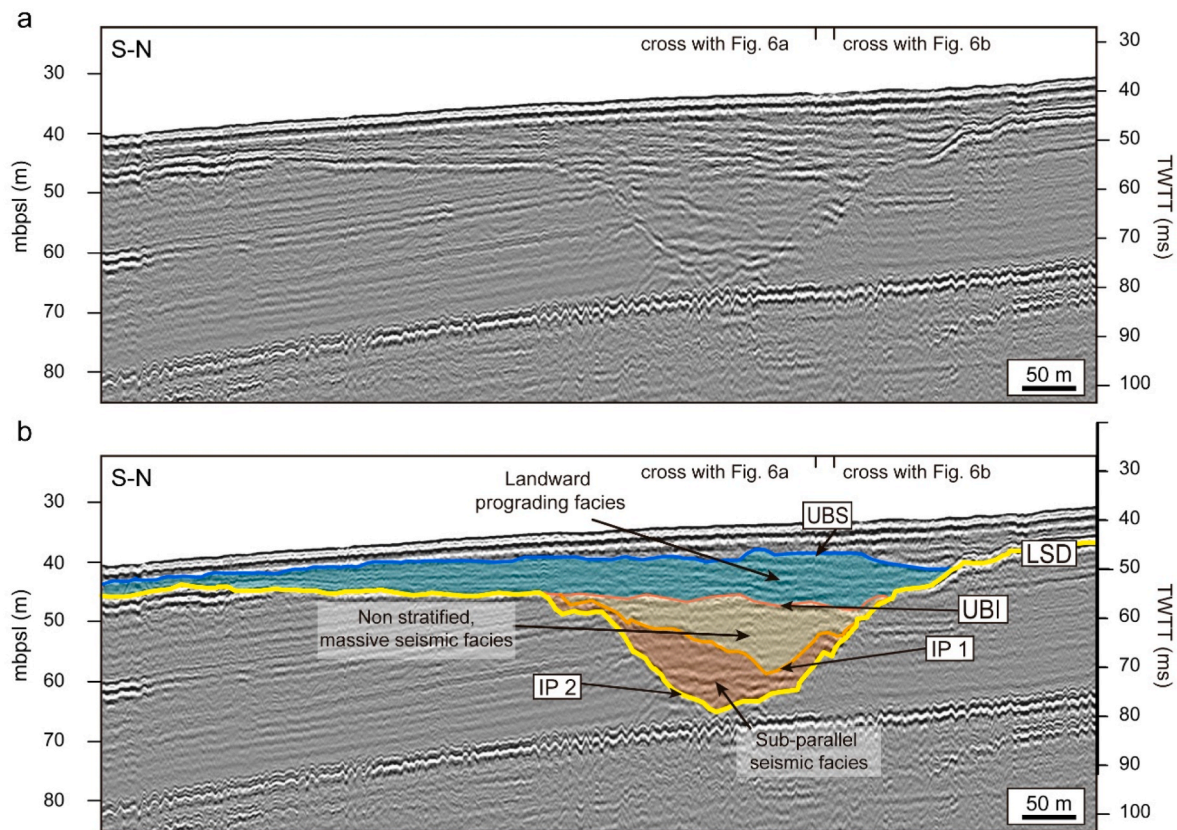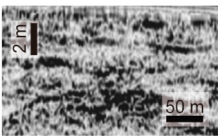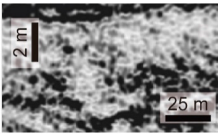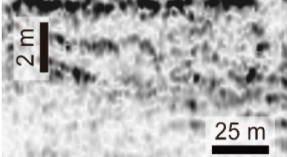
Fig. 8. Downdip cross-shelf (S–N-oriented) Sparker profile showing the main inner-shelf paleovalley (a) and its interpretation (b). The paleovalley occurs landward of the break of slope, and is characterized by two phases of incision and infilling. The second incision phase is asymmetric and is mostly covered by non stratified seismic facies. The reflective unit covering the paleovalley and its infilling is relatively thick here (maximum thickness of 10 m) and exhibits some landward-directed prograding reflectors. The color code and acronyms are indicated in Fig. 4. The location of the seismic section is indicated in Fig. 2 and 7. The crossing with Fig. 6 is also indicated.

Table 2
Summary table of the seismic facies, including the seismic configurations, boundaries, interpretations and acronyms for each seismic unit characterized in the inner shelf paleovalley system identified in this study. IPs 1 and 2: Incised phases 1 and 2; UBI: Upper boundary of infilling; UBS: Upper boundary of sheet-like unit.

Seismic unit	Seismic image	Seismic configuration	Seismic Boundaries	Geometry	Interpretation
Reflective Sheet-like Unit		Amplitude: Low-very low Configuration: semitransparent with high amplitude reflections	Top: UBS Termination: Concordance/Toplap Botom: UBI Termination: Downlap	Wedge	Paleobarrier
ISU 1		Amplitude: Low to medium Configuration: Massive/Chaotic	Top: UBI Termination: Toplap-Erosion Bottom: IP 1 Termination: Concordance/Downlap	Wedge/ Channel-like	Estuarine-mouth massive sands//Tidal Inlet features
ISU 2		Amplitude: Low to medium Configuration: Sub-parallel	Top: IP 1 Termination: Toplap-Erosion Bottom: IP 2 Termination: Concordance/Downlap	Wedge/ Channel-like	Estuarine infilling

Mestdagh et al. (2019), and on other previous studies conducted on the Algarve margin (Hernández-Molina et al., 2016; Luján et al., 2020; Duarte et al., 2022), the following major erosional surfaces have been recognized on the Algarve Shelf: LSD: Last Subaerial Discontinuity (0.02 Ma); LQD: Late Quaternary Discontinuity (0.3 Ma); and MPD: Mid

Pleistocene Discontinuity (0.9 Ma).

The available chronostratigraphic information in the region derived from age-dated major regional seismic surfaces indicates the inner-shelf paleovalley system is genetically related to the LSD (20ka; Mestdagh et al., 2019; Luján et al., 2020), as this surface is the most regionally
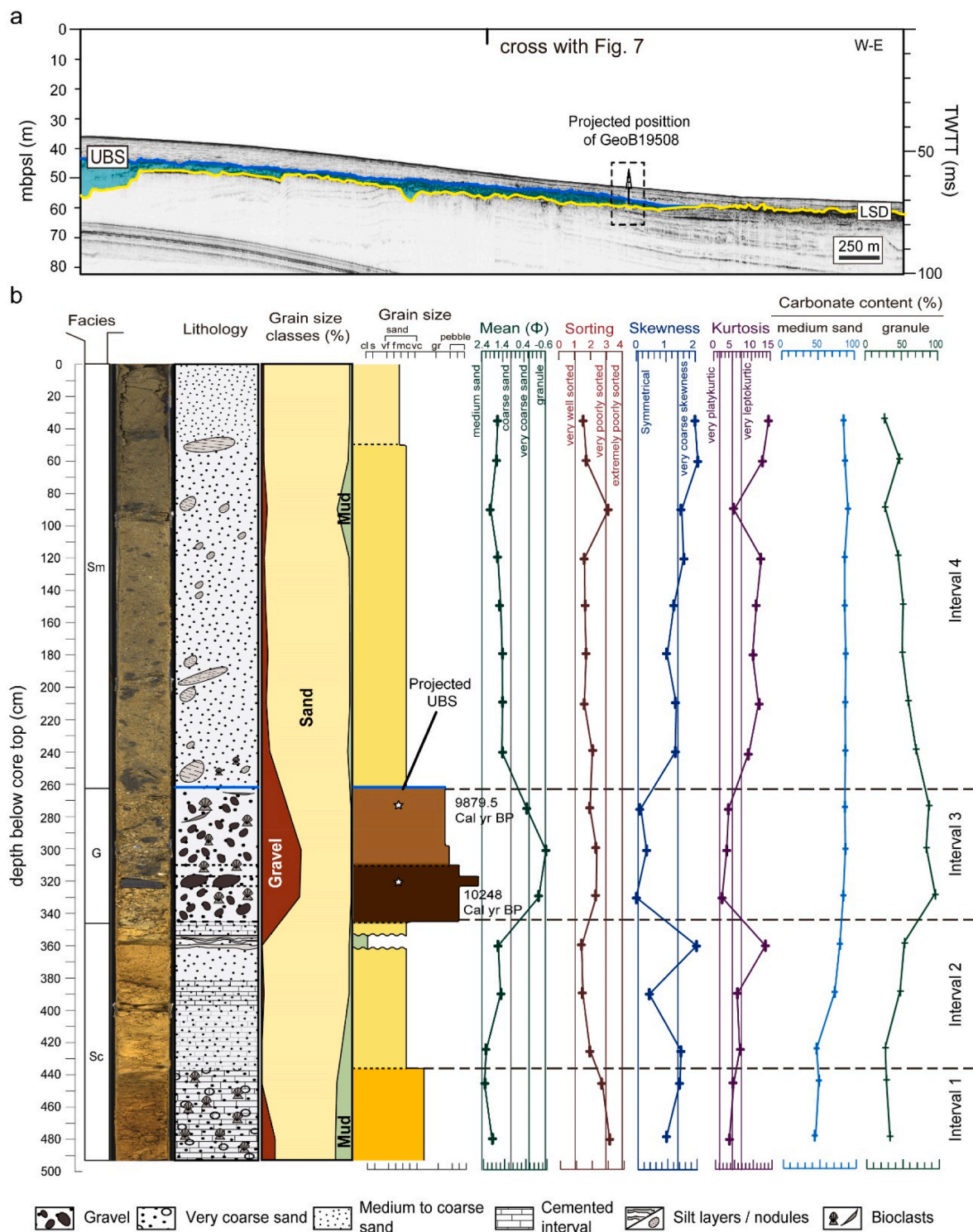
Fig. 9. a) W-E-oriented sub-bottom acoustic profile including the projected position of the studied sediment core GeoB19508. The location of the seismic section is indicated in Fig. 2. The crossing with Fig. 7 is also indicated. b) Photography, facies distribution, lithological description, control age points, grain size statistical parameters (mean, sorting, skewness and kurtosis), and carbonate content of sediment core GeoB19508, characterizing the distal termination of an incised valley. The position of the sediment core is indicated in Fig. 2 and 3.

extensive and can be identified along the entire shelf. Considering the recognition of two main incisions in the different paleovalleys of the inner shelf, two major hypotheses can be proposed:

(a) The paleovalley system is simple, related to a single phase of sea-level fall, and contains a single depositional sequence (Fig. 10b). Equivalent simple incised valleys have been documented elsewhere

(e.g., Allen and Posamentier, 1991, 1994; Li et al., 2002; Gutierrez et al., 2003; Weber et al., 2004a, b). If the inner shelf system is regarded as simple, the older incision phase IP 2 would be related to the prolonged sea-level fall that culminated in the LGM, whereas the whole valley fill would comprise a single depositional sequence deposited after the LGM (Fig. 10b).
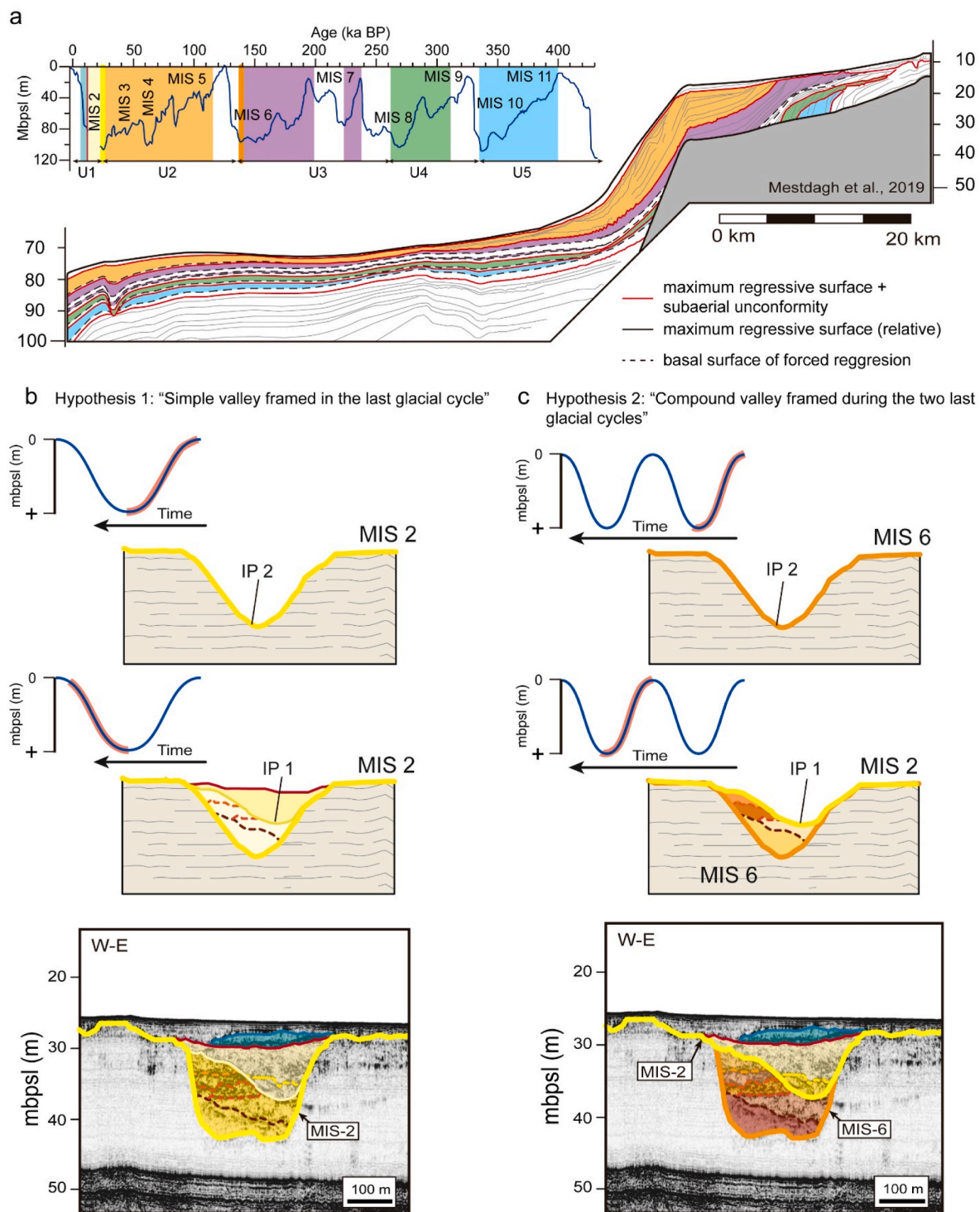
Fig. 10. Synthetic seismic and sequence stratigraphic interpretation for the northern Gulf of Cadiz. a) Late Quaternary sequences and sequence stratigraphic surfaces on the northern Gulf of Cadiz continental margin, from the middle slope to shelf (taken from Mestdagh et al., 2019), and the last 430 ka BP sea-level curve. Marine Isotopic Stages (MIS) 2–11 are highlighted. Colors are according to the proposed hypothesis in this work: post-channel fill deposits: blue; MIS 2-LGM: yellow; MIS 6: orange. b) Schematic model and cross section showing the proposed model for a simple valley framed in the last glacial cycle. c) Schematic model and cross section showing the proposed model for a compound valley framed during the two last glacial cycles.

(b) The paleovalley system is a compound feature, which corresponds to multiple, superimposed cycles of incision and deposition (e.g., Thomas and Anderson, 1994; Foyle and Oertel, 1997; Proust et al., 2001; Tesson et al., 2005). The interpretation of inner shelf system as compound paleovalleys is based in the assumption that incision phases IP 1 and 2 would be related to two different sea-level

falls culminating in two different lowstands (e.g., MIS 2 and MIS 6; Fig. 10c).

The distinction between simple and compound valleys is not straightforward in some cases, and many valleys that were initially interpreted as simple were later reinterpreted as compounds, such as the

cases of the Ria of Vigo, Spain (Martínez-Carreño and García-Gil, 2017), or the Mobile Bay, USA (Greene et al., 2007). Nevertheless, considering the available data, we support the hypotheses of a simple incised-valley model for the inner-shelf system, due to: (a) small incised valley systems tend to form simple architectures and repeated incisions are not favored (Ashley and Sheridan, 1994); in such small valleys, the subaerial exposure and subsequent erosion of the shelf during the LGM would impede the preservation of previous incised features; as analog examples, many incised valleys from the Bay of Biscay, with dimensions comparable to the valleys under scrutiny, are regarded as simple features (e.g., Allen et al., 1970; Allen and Truilhe, 1987; Allen and Posamentier, 1992; Chaumillon, 2008); also, small Mediterranean valleys are also interpreted as simple features (Ronchi et al., 2018; De Falco et al., 2015, 2022); (b) the occurrence of two distinct types of seismic facies within the sedimentary infilling of those inner valleys (Figs. 3–8, 10 b and c) is more compatible with a continuous, simple infilling scenario; (c) the second incision phase is distinctively different from the first one, being less pronounced and strongly asymmetrical in many sections, which is not in agreement with its interpretation as a renewed phase of fluvial erosion.

Assuming the interpretation of a simple valley system, the subsequent infill should have a postglacial age. Considering the proximal location of the paleovalleys, and the fact that the sheet-like reflective unit has been dated between 9880 and 10248 cal yr BP in a distal position off the termination of the paleovalleys, we may infer that at least the second phase of valley infilling and overlying deposits should be Holocene in age, whereas the older estuarine infilling could be pre-Holocene.

5.2. Interpretation of stratigraphic architectures of incised valleys

Most of the paleovalleys identified in the study area exhibit a similar stratigraphic organization, suggesting the common repetition of similar depositional and erosional systems in the different paleovalleys. As explained above, the basal surface of the paleovalleys (IP 2) is interpreted as a fluvial incision associated to a widespread erosional surface, documenting the seaward prolongation of fluvial systems such as the Gilão and Almargem rivers during periods of shelf exposure associated with sea-level lowstands. Equivalent Late Pleistocene fluvial incisions have been documented in numerous inner shelf settings adjacent to minor fluvial networks (e.g., Green, 2009; Green et al., 2013; Ronchi et al., 2018; De Falco et al., 2022).

The lower unit (ISU 2) is characterized by a lack of chaotic facies at the base of the infilling and the dominance of low-to-medium amplitude sub-parallel seismic configurations (Figs. 4 and 5). Similar seismic facies have been interpreted in numerous incised valleys of the Bay of Biscay and the Celtic Sea as estuarine mud and sand alternations mainly composing bay-fill deposits (Reynaud et al., 1999; Weber et al., 2004a; Chaumillon et al., 2008), constituting aggradational phases during periods of sea-level rise (Lericolais et al., 2003). Accordingly, we interpret that the lower unit's facies in the study area may indicate low-energy environments dominated by fine-grained deposits (Fig. 11), pointing to the establishment of estuarine sedimentation during rising sea-level conditions (Figs. 4 and 5). In the main inner-shelf paleovalley, lower sub-parallel facies, ISU 2, are replaced upward by chaotic facies with very irregular boundaries (Figs. 4 and 5). Equivalent erosional, channelized surfaces have been interpreted in the paleo-Etel River as tidal ravinements (Estournès et al., 2012); similarly, we interpret the chaotic facies as tidal estuarine bars modified by tidal ravinement surfaces (Fig. 11). Strong tidal ravinement could also have limited or erased lowstand deposition (Féniès and Lericolais, 2005).

The asymmetric character and lower dimensions of the second phase of incision (IP 1) in many of the incised valleys (Figs. 4–8) is commonly related in the literature with the development of tidal inlets (Ashley and Sheridan, 1994; Dalrymple, 2006; Mattheus and Rodriguez, 2011) or as tidal-related features such as tidal channels (Tessier, 2012) or tidal scours (Graves et al., 2021). The upper unit shows chaotic seismic fabrics with some lateral migration facies (Figs. 4 and 5). The chaotic facies would indicate a change in the depositional environment, as they are typically related with higher-energy environments dominated by coarser sedimentation. Similar infillings could indicate laterally migrating tidal inlet fill deposits (Lericolais et al., 2001) which could be constituted by flood tidal delta deposition (Reynaud et al., 1999). Accordingly, we interpret the transition from moderate amplitude and continuity reflections to chaotic facies as the result of a change in the sedimentary environment during ensuing transgressive conditions, with
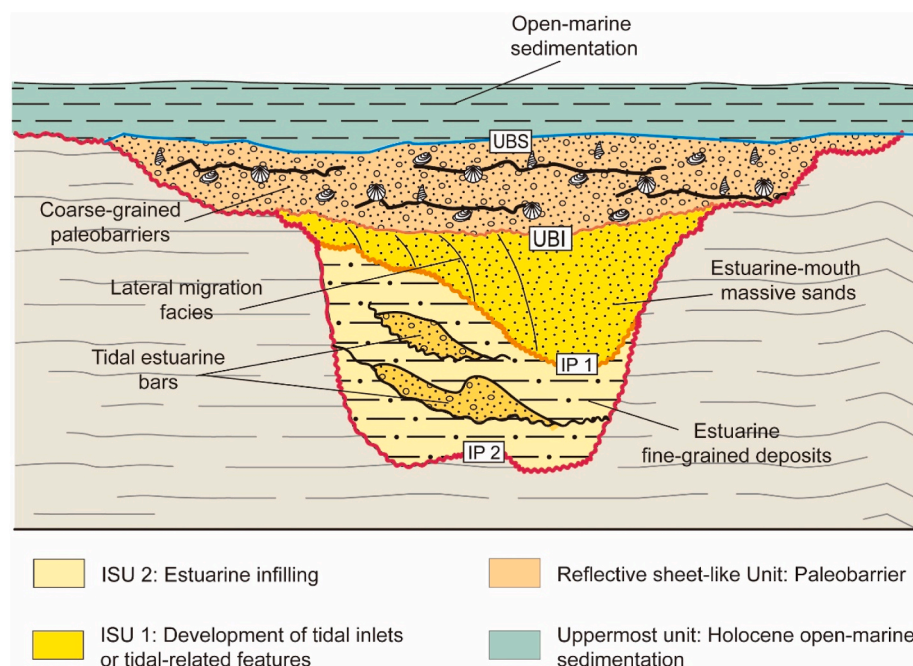

Fig. 11. Idealized stratigraphic model for the incised valleys recognized on the inner shelf of the study area, relating the seismic surfaces and units with their geological interpretation.

deposition of estuarine-mouth massive sands, as documented in other paleovalley systems (Fig. 11; Weber et al., 2004a; Proust et al., 2010; Estournès et al., 2012; Green et al., 2013).

The sheet-like reflective unit may consist of different depositional systems. In the distal termination of the paleovalleys, the occurrence of mounded morphologies at the top of the unit (Fig. 9a) and the strong reflectivity are indicative of submerged coarse-grained paleobarriers, likely extending orthogonal to the trace of the paleovalleys (Fig. 11). Equivalent deposits interpreted as distal barrier-island deposits have been documented during the postglacial evolution of several incised valleys (e.g., Maselli and Trincardi, 2013; Ronchi et al., 2018; De Falco et al., 2022). Sedimentological information supports that interpretation, as the sediment core penetrates the sheet-like reflective unit. The occurrence of cemented intervals (facies Sc) in the lower part of the sediment core (intervals 1 and 2; Fig. 9b) would indicate subaerial sediment exposure. The next interval (interval 3; Fig. 9b) dominated by sandy gravels (facies G) would indicate an increase in environmental energy, possibly related with the formation of the barrier. In more proximal locations, landward-directed progradations locally observed within the reflective unit could be related to depositional systems related to the paleobarriers, such as tidal deltas (e.g., Estournès et al., 2012). Besides, locally the reflective unit exhibits a vertical stacking of tabular deposits, suggesting the landward translation of the system and the generation of a shallower barrier. As those upper deposits are not confined to the valleys, but they extend beyond the banks, their boundaries should be interpreted as wave ravinement surfaces, as documented in some inner-shelf incised valleys in the Bay of Biscay (Chaumillon et al., 2008; Estournès et al., 2012). The uppermost transparent drape observed over the entire study area is interpreted as shelfal, open-marine sedimentation, developed during the Holocene highstand, as documented previously on the Gulf of Cadiz shelf (Fig. 11; Lobo et al., 2004; Hanebuth et al., 2021).

5.3. Driving factors of the paleo-inner-shelf incised valley system

Assuming the above-mentioned preferred genetic scenario for the inner-shelf incised valley system (i.e., simple valley system hypothesis), its subsequent evolution was conditioned by the postglacial sea-level rise; therefore, we interpret that most of the infilling is transgressive in origin. In addition, driving factors such as amount and nature of sediment supply, geological heritage and changing oceanographic regimes should also be considered, as evidenced in other incised valleys (Ashley and Sheridan, 1994; Nordfjord et al., 2005, 2006; Liu et al., 2010; Thanh et al., 2018; Qiu et al., 2019).

5.3.1. Postglacial sea-level changes

The role of rapid postglacial sea-level changes is difficult to evaluate in the studied starved valleys, due to the poor development of transgressive parasequences. In higher supplied incised valleys, postglacial deposits typically exhibit a backstepping pattern. This is the case of the nearby shelf off the Guadiana River, where several postglacial transgressive parasequences have been documented (Carrión-Torrente et al., 2022); their development has been related to periods of reduced sea-level rise between the final phase of meltwater pulse 1A and the Younger Dryas (13.8–11.2 ka), and to periods of high rates of sea-level rise triggered by meltwater pulse 1B during 11.5–8.8 ka.

In other incised valley infillings, coastal barriers have also been formed under different conditions of sea-level rise, either during rapid flooding usually in connection with meltwater pulses (Maselli and Trincardi, 2013; De Falco et al., 2022) or during temporary decelerations of the sea-level rise (Ronchi et al., 2018). In the study area, the ages obtained for the distal barrier unit (i.e., around 10 ka) place its formation during a phase of sustained high rates of sea-level rise (i.e., 130–150 cm/century at around 9.5 ka) after meltwater pulse 1B (Stanford et al., 2011). Landward of the distal barrier, the distribution of the reflective sheet-like unit extending laterally beyond the confines of

the paleovalleys is compatible with a more recent generation of barriers, in fact with limited thickness. Barrier genetic environmental conditions would involve a very rapid transgressive inundation of the paleovalleys, conditioned by the fast sea-level rise after meltwater pulse 1B and the low gradients of the paleo-inner shelf. These conditions, together with scarce fluvial supplies, would account for the limited development of the barriers.

5.3.2. Low sediment supplies

As the relative amounts of fluvial versus estuarine facies seem to be controlled by the rate of sediment supply (Dalrymple et al., 1994), we infer that the lack of representation of fluvial deposits in the inner paleovalleys is a result of low sediment supply related to the low dimensions of the associated fluvial catchments. The relatively low dimensions of the inner valleys also suggest that this system is scaled with the size of the drainage basin; this inference suggests the influence of upstream controls such as water discharge (Mattheus and Rodriguez, 2011; Wang et al., 2019). The dominance of postglacial transgressive deposition in most of the infilling of the inner channels is also compatible with general observations in incised valleys, which argue that lowstand deposition is not favored in small incised valleys (Wang et al., 2020).

The stratigraphic complexity and deposit thickness of the inner paleovalleys in the study area contrast with the paleo-Guadiana incised valley, as explained above; there, coetaneous transgressive intervals appear well-developed showing a set of backstepping parasequences (Lobo et al., 2001, 2005; Carrión-Torrente et al., 2022).

5.3.3. Role of antecedent geology

The absence of related tectonic features together with the minor size of the incisions suggests that the development of paleovalley incisions characterized along the inner shelf off the Gilão-Almargem Estuary was also controlled by antecedent morphology and lithology, which are considered second-order controlling factors, as they influence hydrodynamics and sediment supply in incised valleys (Chaumillon et al., 2010). Our limited data indicate that the identified valleys are narrow and display short cross-shelf extension (Fig. 3; 6–7 km off the present shoreline), indicating limited distal incision; in addition, the trace of the main fluvial valley, which can be considered the seaward extension of the Gilão River as it occurs exactly offshore of the present-day tidal inlet, also disappears in short distances.

Two factors involving antecedent geology and topography may explain the observed distribution of inner-shelf paleovalleys. The first one is the nature of the underlying substratum on the paleo-inner shelf, characterized by widespread highly reflective facies which are suggestive of a coarse-grained sediment composition. This facies could likely represent indurated paleo-barriers, ancient counterparts of the barriers related with the transgressive evolution of the system. This interpretation agrees with reported evidence provided close to the study area, where the distal termination of the main paleovalley of the Guadiana River is also dictated by the occurrence of a coarse-grained inner shelf comprising lithified coastal deposits (Lobo et al., 2018). Therefore, we invoke for the existence of a similar inner-outer shelf distinction along the study area; the paleo-inner shelf would be mainly covered by lithified, indurated deposits, precluding the development of wide fluvial valleys. Seaward of the indurated paleo-inner shelf, finer-grained sediments would be more susceptible to widespread erosion, and the traces of the valleys would be more easily removed. Such control of background geology on the postglacial development of inner incised valley system would be equivalent to the constraints reported in other inner valleys. For example, the course of the Tirso Incised Valley along the Western Sardinia shelf was limited by a barrier system formed at ~9 ka (De Falco et al., 2022).

Another significant topographic feature observed in the study area is a well-marked break of slope on the paleo-inner shelf, delimiting a distal area with higher steepness (>1°). The formation of the break of slope

could be tentatively related to tectonic pulses reported in the northern shelf of the Gulf of Cadiz during the late Quaternary and involving tectonic uplift and enhanced margin progradation (Mestdagh et al., 2019). It has been reported that changes in shelf gradients play a role on initiation and/or enhancement of fluvial incision on the shelf (Klotsko et al., 2021). As most of the incised paleovalleys are limited to the landward, gentler paleo-inner shelf, we propose that the break of slope conditioned the development of the paleovalleys, as they could have been initiated or the incision enhanced when sea level dropped below the feature.

5.3.4. Hydrodynamic regime

In incised valleys, the sedimentation depends on the balance between sediment availability and the potential of hydrodynamics (i.e., waves, tidal currents) to rework the sediments (Tessier, 2012). As we have previously discussed, the potential fluvial inputs for this area are low, attending to the small dimension of the catchment area and the low river sizes. In this context, we need to point out the importance of hydrodynamic as a key mechanism for the development and preservation of this system. As described in other sediment starved margins, such as in the northern and eastern Bay of Biscay, the development of incised valleys system during transgression is driven by two successive processes of sediment reworking: (1) tidal ravinement, when the valley became an estuary and (2) wave ravinement, when the estuary was drowned (Chaumillon et al., 2008).

The paleogeograhic configuration established in the study area during the postglacial transgression could be analogous to the present-day coastal pattern in the Ria Formosa Barrier Island System, characterized by a system of barriers interrupted by tidal inlets, and enclosing landward a system of tidal channels (e.g., Andrade, 1990; Pacheco et al., 2010) (Fig. 12). We propose that wave influence led the generation of barrier systems under an active littoral drift, similarly to the present-day where the net component of sediment transport is directed eastward (e.g., Morales, 1997; Gonzalez et al., 2001). Landward of the barrier, the observed patterns indicate enhanced tidal currents characteristic of small valleys, where the migration of the tidal inlet results in the creation of a tidal ravinement (Ashley and Sheridan, 1994). The recognition of paleotidal inlets/channels in several channels would agree with a major reoccupation of previous incised valleys by tidal channels (Fig. 12). Despite of low sediment inputs, the occurrence of sands within the valleys implies the activity of hydrodynamic processes such as tidal currents that have been effective transporting coarse-grained sediments and have led to a valley fill dominated by tidal related deposits (Fig. 12), such as estuarine tidal bars observed in the older phase of valley infilling, estuarine-mouth sand plough in the younger phase of valley infilling, and local tidal deltas/tidal mouth deposits associated to the barriers. Equivalent tidal deposits have been reported in other valley infillings (Féniès and Lericolais, 2005; Chaumillon et al., 2008). Those observations would indicate that the postglacial evolution of the inner system seems to have been influenced by both tidal- and wave-dominated processes, as at least local tidal influence extends landward of the tidal inlets (Tessier, 2012). Therefore, this system can be considered as mixed sensu Dalrymple et al. (1992) and Chaumillon
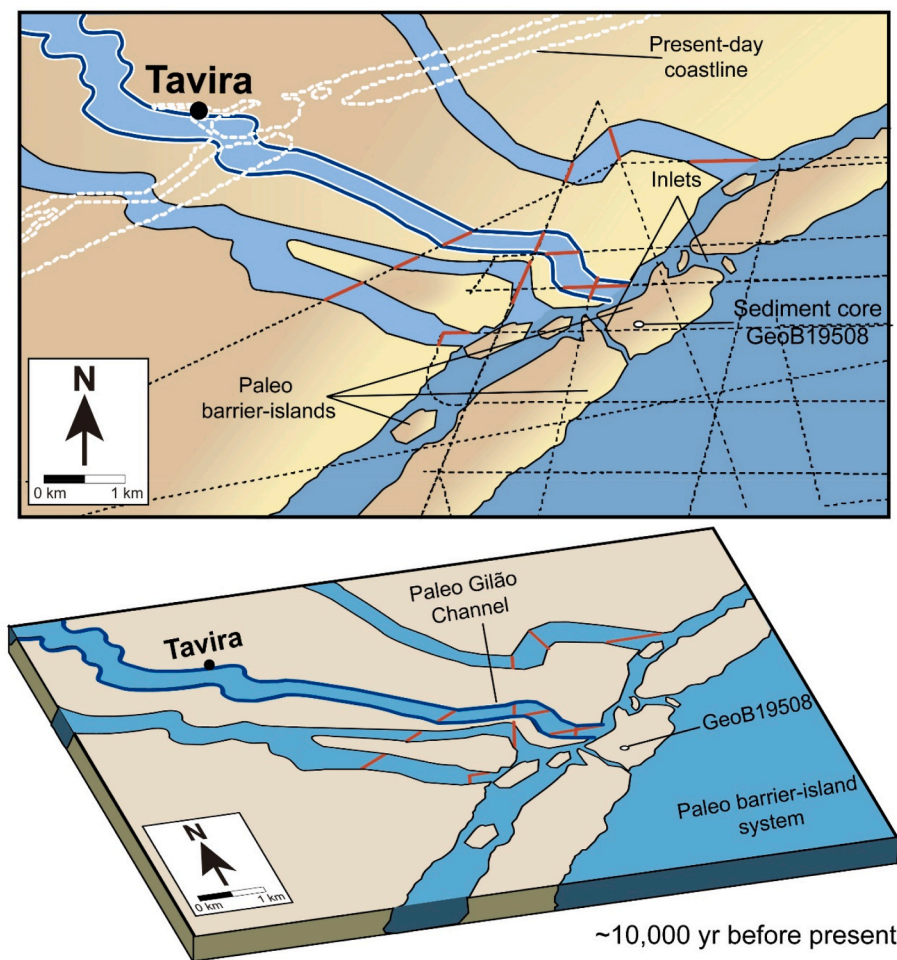

Fig. 12. Proposed paleogeographic reconstruction of the study area at ~10 ka BP where multiple sandy islands are interrupted by numerous tidal inlets in several channels showing a coastal pattern which is similar to that of the present-day Ria Formosa Barrier Island System. The position of seismic lines and the studied sediment core are indicated and the red lines correspond with the width of IP 1 along the different incised valleys.

et al. (2010).

6. Conclusions

Seismic stratigraphic evidence correlated with age-constraint regional stratigraphic horizons and limited recent sediment data have revealed the existence of a network of incised valleys off the Gilão-Almargem Estuary, a small fluvial drainage system in the eastern Algarve shelf, northern margin of the Gulf of Cadiz. The occurrence of such sediment routing system mostly limited to the paleo-inner shelf likely reveals the operation of distinct driving factors modulating the primary glacio-eustatic factor, usually considered as the primary control on incised-valley development, and enabling the formation of abundant incised valleys in a currently low supply setting.

The dendritic inner-shelf valley network shows no signs of tectonic control. A number of stratigraphic evidences drive us to interpret the inner-shelf paleovalleys as a simple system formed during the last glacial cycle; fluvial incision is likely to have been occurred during falling sea levels leading into the Last Glacial Maximum, whereas the incised valley infill took place during the postglacial transgression. The stratigraphic architecture reveals the frequent occurrence of coarse-grained sediment bodies like estuarine bars, estuary-mouth sand plough and coastal barriers, and a second phase of incision interpreted as tidal inlets/channels. Its inner location strongly suggests that at least the recent phase of infilling is Holocene in age.

The formation of the inner shelf paleovalleys was strongly determined by background geology, where the occurrence of a flat, lithified paleo-inner shelf bounded seaward by a break of slope conditioned the formation of small-sized incised valleys. Subsequently, the infilling of the valleys took place under a context of high rates of sea-level rise and limited fluvial supply at the start of the Holocene. The paleogeographic configuration during this final phase of the postglacial transgression likely involved the development of a dendritic system, with numerous barriers interrupted by tidal inlets or scours in a mixed estuarine system.

Declaration of competing interest

The authors declare that they have no known competing financial interests or personal relationships that could have appeared to influence the work reported in this paper.

Acknowledgements

References

Allen, G.P., Castaing, P., Feral, A., Klingebiel, A., Vigneaux, M., 1970. Contribution à l'étude des facies de comblement et interprétation paléogéographique de l'évolution des milieux sédimentaires récents et actuels de l'estuaire de la Gironde. Bull. Inst. Geol. Bassin Aquitaine 8, 99–155.

Allen, G.P., Posamentier, H.W., 1991. Facies and the stratal patterns in incised valleys: examples form the recent Gironde Estuary (France) and the Cretaceous Viking Formation. Am. Assoc. Petr. Geol., annual Meeting, Program with Abstract 534.

Allen, G.P., Posamentier, H.W., 1992. On the Origin and Subsequent Modification of Incised Valleys. Am. Assoc. Petr. Geol., annual convention, abstracts with programs, Calgary, Canada, p. 70.

Allen, G.P., Posamentier, H.W., 1994. Transgressive facies and sequence architecture in mixed tide and wave-dominated incised valleys: example from the Gironde estuary, France. In: Dalrymple, R.W., Boyd, R.J., Zaitlin, B.A. (Eds.), Incised-valley Systems: Origin and Sedimentary Sequences, vol. 51. SEPM Spec, pp. 225–240. https://doi.org/10.2110/pec.94.12.0225.

Allen, G.P., Truilhe, G., 1987. Stratigraphic and facies model of a transgressive estuarine valley fill in the Gironde estuary (France). In: James, D.P., Leckie, D.A. (Eds.), Sequences, Stratigraphy, Sedimentology Surface and Subsurface, vol. 15. Can. Soc. Pet. Geol. Mem., p. 575

Andrade, C., 1990. O ambiente de barreira da Ria Formosa (Algarve, Portugal). Unpublished PhD dissertation, Department of Geology, Univ. Lisbon, p. 645.

Aquino da Silva, A.G., Stattegger, K., Schwarzer, K., Vital, H., 2016. Seismic stratigraphy as indicator of late Pleistocene and Holocene Sea level changes on the NE Brazilian continental shelf. J. S. Am. Earth Sci. 70, 188–197. https://doi.org/10.1016/j.jsames.2016.05.001.

Ashley, G.M., Sheridan, R.E., 1994. Depositional model for valley fills on a passive continental margin. In: Dalrymple, R.W., Boyd, R.J., Zaitlin, B.A. (Eds.), Incised-valley Systems: Origin and Sedimentary Sequences, vol. 51. SEPM Spec. https://doi.org/10.2110/pec.94.12.0285.

Baldy, P., 1977. Géologie du plateau continental portugaise (au sud du cap de Sines). Thèse de 3ème Cycle. Université Paris VI, p. 113pp.

Bellanco, M.J., Sánchez-Leal, R.F., 2016. Spatial distribution and intra-annual variability of water masses on the eastern Gulf of Cadiz seabed. Continent. Shelf Res. 128, 26–35. https://doi.org/10.1016/j.csr.2016.09.001.

Blum, M., Martin, J., Milliken, K., Garvin, M., 2013. Paleovalley systems: insights from Quaternary analogs and experiments. Earth Sci. Rev. 116, 128–169. https://doi.org/10.1016/j.earscirev.2012.09.003.

Boski, T., Camacho, S., Moura, D., Fletcher, W., Wilamowski, A., Veiga-Pires, C., Correia, V., Loureiro, C., Santana, P., 2008. Chronology of the sedimentary processes during the postglacial sea level rise in two estuaries of the Algarve coast, Southern Portugal. Estuar. Coast Shelf Sci. 77, 230–244. https://doi.org/10.1016/j.ecss.2007.09.012.

Bosnic, I., Cascalho, J., Taborda, R., Drago, T., Hermínio, J., Rosa, M., Dias, J., Garel, E., 2017. Nearshore sediment transport: coupling sand tracer dynamics with oceanographic forcing. Mar. Geol. 385, 293–303. https://doi.org/10.1016/j.margeo.2017.02.004.

Boyd, R., Dalrymple, R., Zaitlin, B., 2006. Estuarine and incised-valley facies models. In: Posamentier, H.W., Walker, R.G. (Eds.), Facies Models Revisited, vol. 84. SEPM Spec, pp. 171–235. https://doi.org/10.2110/pec.06.84.0171.

Burger, R.L., Fulthorpe, C.S., Austin, J.A., 2001. Late Pleistocene channel incisions in the southern Eel River Basin, northern California: implications for tectonic vs. eustatic influences on shelf sedimentation patterns. Mar. Geol. 177, 317–330. https://doi.org/10.1016/S0025-3227(01)00166-9.

Carrión-Torrente, Á., Lobo, F.J., Puga-Bernabéu, Á., Mendes, I., Lebreiro, S., García, M., van Rooij, D., Luján, M., Reguera, M.I., Antón, L., 2022. Episodic postglacial deltaic pulses in the Gulf of Cadiz: implications for the development of a transgressive shelf and driving environmental conditions. J. Sediment. Res. 92, 1116–1140. https://doi.org/10.2110/jsr.2021.110.

Catuneanu, O., Galloway, W.E., Kendall, C.G.S.C., Miall, A.D., Posamentier, H.W., Strasser, A., Tucker, M.E., 2011. Sequence stratigraphy: methodology and nomenclature. Newsl. Stratigr. 44, 173–245. https://doi.org/10.1127/0078-0421/2011/0011.

Chaumillon, E., Weber, N., 2006. Spatial variability of modern incised valleys on the French atlantic coast : comparison between the charente (pertuis d'Antioche) and the lay-sèvre (pertuis Breton) incised-valleys. In: Dalrymple, R.W., Leckie, D.A., Tillman, R.W. (Eds.), Incised Valleys in Time and Space, vol. 85. SEPM Spec, pp. 57–85. https://doi.org/10.2110/pec.06.85.0057.

Chaumillon, E., Proust, J.N., Menier, D., Weber, N., 2008. Incised-valley morphologies and sedimentary-fills within the inner shelf of the Bay of Biscay (France): a synthesis. J. Mar. Syst. 72, 383–396. https://doi.org/10.1016/j.jmarsys.2007.05.014.

Chaumillon, E., Tessier, B., Reynaud, J.-Y., 2010. Stratigraphic records and variability of incised valleys and estuaries along French coasts. Bull. Soc. Geol. Fr. 181, 75–85. https://doi.org/10.2113/gssgfbull.181.2.75.

Ciavola, P., Taborda, R., Ferreira, Ó., Dias, J.A., 1997. Field measurements of longshore sand transport and control processes on a steep meso-tidal beach in Portugal. J. Coast Res. 13, 1119–1129.

Dalrymple, R.W., 2006. Incised Valleys in Time and Space: an Introduction to the volume and an examination of the controls on valley formation and filling. In: Dalrymple, R. W., Leckie, D.A., Tillman, R.W. (Eds.), Incised Valleys in Time and Space, vol. 85. SEPM Spec, pp. 5–12. https://doi.org/10.2110/pec.06.85.0005.

Dalrymple, R.W., Zaitlin, B.A., Boyd, R., 1992. Estuarine facies models; conceptual basis and stratigraphic implications. J. Sediment. Res. 62, 1130–1146. https://doi.org/10.1306/D4267A69-2B26-11D7-8648000102C1865D.

Dalrymple, R.W., Boyd, R., Zaitlin, B.A., 1994. Incised-Valley Systems: Origin and Sedimentary Sequences, vol. 51. SEPM Spec, p. 391p. https://doi.org/10.2110/pec.94.12.

De Falco, G., Antonioli, F., Fontolan, G., Lo Presti, V., Simeone, S., Tonielli, R., 2015. Early cementation and accommodation space dictate the evolution of barrier system during the Holocene. Mar. Geol. 369, 52–66. https://doi.org/10.1016/j.margeo.2015.08.002.

De Falco, G., Carannante, A., Del Vais, C., Gasperini, L., Pascucci, V., Sanna, I., Simeone, S., Conforti, A., 2022. Evolution of a single incised valley related to inherited geology, sea level rise and climate changes during the Holocene (Tirso

river, Sardinia, western Mediterranean Sea). Mar. Geol. 451, 106885 https://doi.org/10.1016/j.margeo.2022.106885.

Del Río, L., Plomaritis, T.A., Benavente, J., Valladares, M., Ribera, P., 2012. Establishing storm thresholds for the Spanish Gulf of Cádiz coast. Geomorphology 143–144, 13–23. https://doi.org/10.1016/j.geomorph.2011.04.048.

Dolbeth, M., Ferreira, Ó., Teixeira, H., Marques, J.C., Dias, J.A., Pardal, M.A., 2007. Beach morphodynamic impact on a macrobenthic community along a subtidal depth gradient. Mar. Ecol. Prog. Ser. 352, 113–124. https://doi.org/10.3354/meps07040.

Duarte, D., Roque, C., Ng, Z.L., Hernández-Molina, F.J., Magalhães, V.H., Silva, S., Llave, E., 2022. Structural control and tectono-sedimentary evolution of the Gulf of Cadiz, SW Iberia since the late Miocene: implications for contourite depositional system. Mar. Geol. 449, 106818 https://doi.org/10.1016/j.margeo.2022.106818.

EMODnet Bathymetry Consortium, 2020. EMODnet digital bathymetry (DTM). EMODnet bathymetry Consortium. https://doi.org/10.12770/bb6a87dd-e579-4036-abe1-e649cea9881a.

Estournès, G., Menier, D., Guillocheau, F., Le Roy, P., Paquet, F., Goubert, E., 2012. The paleo-Etel River incised valley on the Southern Brittany inner shelf (Atlantic coast, France): preservation of Holocene transgression within the remnant of a middle Pleistocene incision? Mar. Geol. 329–331, 75–92. https://doi.org/10.1016/j.margeo.2012.08.005.

Féniès, H., Lericolais, G., 2005. Architecture interne d'une vallée incisée sur une côte à forte énergie de houle et de marée (vallée de la Leyre, côte aquitaine, France). C. R. Geosci. 337, 1257–1266. https://doi.org/10.1016/j.crte.2005.06.005.

Fernández-Salas, L.M., Rey, J., Pérez-Vazquez, E., Ramírez, J.L., Hernández-Molina, F.J., Somoza, L., De Andrés, J.R., Lobo, F.J., 1999. Morphology and characterization of the relict facies on the internal continental shelf in the Gulf of Cadiz between Ayamonte and Huelva (Spain). Bol. Inst. Esp. Oceanogr. 15, 123–132.

Foyle, A.M., Oertel, G.F., 1997. Transgressive systems tract development and incised-valley fills within a Quaternary estuary shelf system: Virginia inner shelf, USA. Mar. Geol. 137 (3–4), 227–249. https://doi.org/10.1016/S0025-3227(96)00092-8.

Folk, R.L., 1954. The distinction between grain size and mineral composition in sedimentary-rock nomenclature. J. Geol. 62 (4), 344–359. https://www.jstor.org/stable/30065016.

Garcia, T., Ferreira, Ó., Matias, A., Dias, J.A., 2002. Recent evolution of culatra island (Algarve–Portugal). In: Gomes, F.V., Taveira Pinto, F., das Neves, L. (Eds.), Littoral 2002: 6th International Symposium Proceedings: a Multi-Disciplinary Symposium on Coastal Zone Research-Management and Planning: Proceedings. Porto, pp. 289–294.

García-Lafuente, J., Delgado, J., Criado-Aldeanueva, F., Bruno, M., del Río, J., Miguel Vargas, J., 2006. Water mass circulation on the continental shelf of the Gulf of Cádiz. Deep Sea Res. Part II Top. Stud. Oceanogr. 53, 1182–1197. https://doi.org/10.1016/j.dsr2.2006.04.011.

Garel, E., Laiz, I., Drago, T., Relvas, P., 2016. Characterisation of coastal counter-currents on the inner shelf of the Gulf of Cádiz. J. Mar. Syst. 155, 19–34. https://doi.org/10.1016/j.jmarsys.2015.11.001.

Gomes, M.P., Vital, H., Stattegger, K., Schwarzer, K., 2016. Bedrock control on the assu Incised Valley morphology and sedimentation in the Brazilian equatorial shelf. Int. J. Sediment Res. 31, 181–193. https://doi.org/10.1016/j.ijsrc.2015.04.002.

Gonzalez, R., Dias, J.A., Ferreira, Ó., 2001. Recent rapid evolution of the Guadiana estuary mouth (southwestern iberian peninsula). J. Coast Res. 516–527. http://www.jstor.org/stable/25736317.

Gonzalez, R., Dias, J.A., Lobo, F., Mendes, I., 2004. Sedimentological and paleoenvironmental characterisation of transgressive sediments on the Guadiana shelf (northern gulf of Cadiz, SW iberia). Quat. Int. 120, 133–144. https://doi.org/10.1016/j.quaint.2004.01.012.

Graves, L.G., Driscoll, N.W., Maloney, J.M., 2021. Tectonic and eustatic control on channel formation, erosion, and deposition along a strike-slip margin, San Diego, California, USA. Continent. Shelf Res. 231, 104571 https://doi.org/10.1016/j.csr.2021.104571.

Green, A.N., 2009. Palaeo-drainage, incised valley fills and transgressive systems tract sedimentation of the northern KwaZulu-Natal continental shelf, South Africa, SW Indian Ocean. Mar. Geol. 263, 46–63. https://doi.org/10.1016/j.margeo.2009.03.017.

Green, A.N., Dladla, N., Garlick, G.L., 2013. Spatial and temporal variations in incised valley systems from the Durban continental shelf, KwaZulu-Natal, South Africa. Mar. Geol. 335, 148–161. https://doi.org/10.1016/j.margeo.2012.11.002.

Greene, D.L., Rodriguez, A.B., Anderson, J.B., 2007. Seaward-branching coastal-plain and piedmont incised-valley systems through multiple sea-level cycles: late Quaternary examples from Mobile Bay and Mississippi Sound. U.S.A. J. Sediment. Res. 77, 139–158. https://doi.org/10.2110/jsr.2007.016.

Gutierrez, B.T., Uchupi, E., Driscoll, N.W., Aubrey, D.G., 2003. Relative sea-level rise and the development of valley-fill and shallow water sequences in Nantucket sound, Massachusetts. Mar. Geol. 193 (3–4), 295–314. https://doi.org/10.1016/S0025-3227(02)00665-5.

Hanebuth, T.J.J., Lee, M., Lobo, F.J., Mendes, I., 2021. Formation history and material budget of holocene shelf mud depocenters in the Gulf of Cadiz. Sediment. Geol. 421, 105956 https://doi.org/10.1016/j.sedgeo.2021.105956.

Heaton, T.J., Köhler, P., Butzin, M., Bard, E., Reimer, R.W., Austin, W.E.N., Bronk Ramsey, C., Grootes, P.M., Hughen, K.A., Kromer, B., Reimer, P.J., Adkins, J., Burke, A., Cook, M.S., Olsen, J., Skinner, L.C., 2020. Marine20-the marine radiocarbon age calibration curve (0-55,000 cal BP). Radiocarbon 62, 779–820. https://doi.org/10.1017/RDC.2020.68.

Hernández-Molina, F.J., Fernández-Salas, L.M., Lobo, F., Somoza, L., Díaz-del-Río, V., Alveirinho Dias, J.M., 2000. The infralittoral prograding wedge: a new large-scale progradational sedimentary body in shallow marine environments. Geo Mar. Lett. 20, 109–117. https://doi.org/10.1007/s003670000040.

Hernández-Molina, F.J., Somoza, L., Vázquez, J.T., Lobo, F., Fernández-Puga, M.C., Llave, E., Díaz-del-Río, V., 2002. Quaternary stratigraphic stacking patterns on the continental shelves of the southern Iberian Peninsula: their relationship with global climate and palaeoceanographic changes. Quat. Int. 92, 5–23. https://doi.org/10.1016/S1040-6182(01)00111-2.

Hernández-Molina, F.J., Llave, E., Stow, D.A.V., Garcia, M., Somoza, L., Vazquez, J.T., Lobo, F.J., Maestro, A., del Rio, V.D., Leon, R., Medialdea, T., Gardner, J., 2006. The contourite depositional system of the Gulf of Cadiz: a sedimentary model related to the bottom current activity of the Mediterranean outflow water and its interaction with the continental margin. Deep. Sea. Res. Part 2. Top. Stud. Oceanogr. 53 (11–13), 1420–1463. https://doi.org/10.1016/j.dsr2.2006.04.016.

Hernández-Molina, F.J., Sierro, F.J., Llave, E., Roque, C., Stow, D.A.V., Williams, T., Lofi, J., Van der Schee, M., Arnáiz, A., Ledesma, S., Rosales, C., Rodríguez-Tovar, F. J., Pardo-Igúzquiza, E., Brackenridge, R.E., 2016. Evolution of the gulf of Cadiz margin and southwest Portugal contourite depositional system: tectonic, sedimentary and paleoceanographic implications from IODP expedition 339. Mar. Geol. 377, 7–39. https://doi.org/10.1016/j.margeo.2015.09.013.

Klotsko, S., Skakun, M., Maloney, J., Gusick, A., Davis, L., Nyers, A., Ball, D., 2021. Geologic controls on paleodrainage incision and morphology during sea level lowstands on the Cascadia shelf in Oregon. USA. Mar. Geol. 434, 106444 https://doi.org/10.1016/j.margeo.2021.106444.

Lericolais, G., Berné, S., Féniès, H., 2001. Seaward pinching out and internal stratigraphy of the gironde incised valley on the shelf (bay of Biscay). Mar. Geol. 175, 183–197. https://doi.org/10.1016/S0025-3227(01)00134-7.

Lericolais, G., Auffret, J.P., Bourillet, J.F., 2003. The quaternary channel river: seismic stratigraphy of its palaeo-valleys and deeps. J. Quat. Sci. 18, 245–260. https://doi.org/10.1002/jqs.759.

Li, C., Wang, P., Sun, H., Zhang, J., Fan, D., Deng, B., 2002. Late Quaternary incised-valley fill of the Yangtze delta (China): its stratigraphic framework and evolution. Sediment. Geol. 152, 133–158. https://doi.org/10.1016/S0037-0738(02)00066-0.

Liu, J., Saito, Y., Kong, X., Wang, H., Wen, C., Yang, Z., Nakashima, R., 2010. Delta development and channel incision during marine isotope stages 3 and 2 in the western South Yellow Sea. Mar. Geol. 278, 54–76. https://doi.org/10.1016/j.margeo.2010.09.003.

Lobo, F.J., Hernández-Molina, F.J., Somoza, L., Rodero, J., Maldonado, A., Barnolas, A., 2000. Patterns of bottom current flow deduced from dune asymmetries over the Gulf of Cadiz shelf (southwest Spain). Mar. Geol. 164, 91–117. https://doi.org/10.1016/S0025-3227(99)00132-2.

Lobo, F.J., Hernández-Molina, F.J., Somoza, L., Díaz del Río, V., 2001. The sedimentary record of the post-glacial transgression on the Gulf of Cadiz continental shelf (Southwest Spain). Mar. Geol. 178, 171–195. https://doi.org/10.1016/S0025-3227(01)00176-1.

Lobo, F.J., Sánchez, R., González, R., Dias, J.M.A., Hernández-Molina, F.J., Fernández-Salas, L.M., Díaz Del Río, V., Mendes, I., 2004. Contrasting styles of the Holocene highstand sedimentation and sediment dispersal systems in the northern shelf of the Gulf of Cadiz. Continent. Shelf Res. 24, 461–482. https://doi.org/10.1016/j.csr.2003.12.003.

Lobo, F.J., Fernández-Salas, L.M., Hernández-Molina, F.J., González, R., Dias, J.M.A., Díaz Del Río, V., Somoza, L., 2005. Holocene highstand deposits in the Gulf of Cadiz, SW Iberian Peninsula: a high-resolution record of hierarchical environmental changes. Mar. Geol. 219, 109–131. https://doi.org/10.1016/j.margeo.2005.06.005.

Lobo, F.J., García, M., Luján, M., Mendes, I., Reguera, M.I., Van Rooij, D., 2018. Morphology of the last subaerial unconformity on a shelf: insights into transgressive ravinement and incised valley occurrence in the Gulf of Cádiz. Geo Mar. Lett. 38, 33–45. https://doi.org/10.1007/s00367-017-0511-9.

Lopes, F.C., Cunha, P.P., le Gall, B., 2006. Cenozoic seismic stratigraphy and tectonic evolution of the Algarve margin (offshore Portugal, southwestern Iberian Peninsula). Mar. Geol. 231 (1–4), 1–36. https://doi.org/10.1016/j.margeo.2006.05.007.

Luján, M., Lobo, F.J., Mestdagh, T., Vázquez, J.T., Fernández-Puga, M.C., Van Rooij, D., 2020. Pliocene-Quaternary deformational structures in the eastern Algarve continental shelf, Gulf of Cadiz. Geogaceta 67, 3–6.

Maldonado, A., Nelson, C.H., 1999. Interaction of tectonic and depositional processes that control the evolution of the Iberian Gulf of Cadiz margin. Mar. Geol. 155 (1–2), 217–242. https://doi.org/10.1016/S0025-3227(98)00148-0.

Maldonado, A., Rodero, J., Pallarés, L., Pérez, L., Somoza, L., Medialdea, T., Hernández-Molina, F.J., Lobo, F.J., 2003. Mapa Geológico de la Plataforma Continental Española y Zonas Adyacentes. Escala 1:200.000. Cádiz. Instituto Geológico y Minero de España, Madrid.

Martínez-Carreño, N., García-Gil, S., 2017. Reinterpretation of the Quaternary sedimentary infill of the Ría de Vigo, NW Iberian Peninsula, as a compound incised valley. Quat. Sci. Rev. 173, 124–144. https://doi.org/10.1016/j.quascirev.2017.08.015.

Maselli, V., Trincardi, F., 2013. Large-scale single incised valley from a small catchment basin on the western Adriatic margin (central Mediterranean Sea). Global Planet. Change 100, 245–262. https://doi.org/10.1016/j.gloplacha.2012.10.008.

Mattheus, C.R., Rodriguez, A.B., 2011. Controls on late quaternary incised-valley dimension along passive margins evaluated using empirical data. Sedimentology 58, 1113–1137. https://doi.org/10.1111/j.1365-3091.2010.01197.x.

Menier, D., Tessier, B., Proust, J.N., Baltzer, A., Sorrel, P., Traini, C., 2010. The Holocene transgression as recorded by incised-valley infilling in a rocky coast context with low sediment supply (southern Brittany, western France). Bull. Soc. Geol. Fr. 181, 115–128. https://doi.org/10.2113/gssgfbull.181.2.115.

Mestdagh, T., Lobo, F.J., Llave, E., Hernández-Molina, F.J., Van Rooij, D., 2019. Review of the late Quaternary stratigraphy of the northern Gulf of Cadiz continental margin: new insights into controlling factors and global implications. Earth Sci. Rev. 198, 102944 https://doi.org/10.1016/j.earscirev.2019.102944.

Mitchum Jr., R.M., 1977. Seismic stratigraphy and global changes of sea level. Part 11: glossary of terms used in seismic stratigraphy. In: Payton, C.E. (Ed.), Seismic Stratigraphy e Applications to Hydrocarbon Exploration, vol. 26. AAPG Memoir, pp. 205–212.

Morales, J.A., 1997. Evolution and facies architecture of the mesotidal Guadiana River delta (S.W. Spain-Portugal). Mar. Geol. 138 (1–2), 127–148. https://doi.org/10.1016/S0025-3227(97)00009-1.

Nelson, C.H., Baraza, J., Maldonado, A., Rodero, J., Escutia, C., Barber Jr., J.H., 1999. Influence of the Atlantic inflow and Mediterranean outflow currents on Late Quaternary sedimentary facies of the Gulf of Cadiz continental margin. Mar. Geol. 155, 99–129. https://doi.org/10.1016/S0025-3227(98)00143-1.

Nordfjord, S., Goff, J.A., Austin Jr., J.A., Sommerfield, C.K., 2005. Seismic geomorphology of buried channel systems on the New Jersey outer shelf: assessing past environmental conditions. Mar. Geol. 214, 339–364. https://doi.org/10.1016/j.margeo.2004.10.035.

Nordfjord, S., Goff, J.A., Austin, J.A., Gulick, S.P.S., 2006. Seismic facies of incised-valley fills, New Jersey continental shelf: implications for erosion and preservation acting during latest Pleistocene-Holocene transgression. J. Sediment. Res. 76, 1284–1303. https://doi.org/10.2110/jsr.2006.108.

Pacheco, A., Ferreira, Ó., Williams, J.J., Garel, E., Vila-Concejo, A., Dias, J.A., 2010. Hydrodynamics and equilibrium of a multiple-inlet system. Mar. Geol. 274, 32–42. https://doi.org/10.1016/j.margeo.2010.03.003.

Paquet, F., Menier, D., Estournès, G., Bourillet, J.F., Leroy, P., Guillocheau, F., 2010. Buried fluvial incisions as a record of middle-late Miocene eustasy fall on the armorican shelf (bay of Biscay, France). Mar. Geol. 268, 137–151. https://doi.org/10.1016/j.margeo.2009.11.002.

Pilkey, O., Neal, W., Monteiro, J., Dias, J., 1989. Algarve barrier islands: a noncoastal-plain system in Portugal. J. Coast Res. 5 (2), 239–261. http://www.jstor.org/stable/4297527.

Plomaritis, T.A., Benavente, J., Laiz, I., Del Río, L., 2015. Variability in storm climate along the Gulf of Cadiz: the role of large scale atmospheric forcing and implications to coastal hazards. Clim. Dynam. 45, 2499–2514. https://doi.org/10.1007/s00382-015-2486-4.

Posamentier, H.W., Vail, P.R., 1988. Eustatic controls on clastic deposition, II: sequence and systems tract models. In: Wilgus, C.K., Hastings, B.S., Kendall, C.G.StC., Posamentier, H.W., Ross, C.A., Van Wagoner, J.C. (Eds.), Sea Level Changes: an Integrated Approach, vol. 42. SEPM Spec, pp. 125–154. https://doi.org/10.2110/pec.88.01.0125.

Proust, J.N., Menier, D., Guillocheau, F., Guennoc, P., Bonnet, S., Rouby, D., Le Corre, C., 2001. Les vallées fossiles de la baie de la Vilaine: nature et évolution du prisme sédimentaire côtier du Pleistocène armoricain. Bull. Soc. Géol. Fr. 172 (6), 737–749.

Proust, J.N., Renault, M., Guennoc, P., Thinon, I., 2010. Sedimentary architecture of the Loire River drowned valleys of the French Atlantic shelf. Bull. Soc. Géol. Fr. 181, 129–149. https://doi.org/10.2113/gssgfbull.181.2.129.

Qiu, J., Liu, Jian, Saito, Y., Yin, P., Zhang, Y., Liu, Jinqing, Zhou, L., 2019. Seismic morphology and infilling architecture of incised valleys in the northwest South Yellow Sea since the last glaciation. Continent. Shelf Res. 179, 52–65. https://doi.org/10.1016/j.csr.2019.04.008.

Ramos, A., Fernández, O., Terrinha, P., Muñoz, J.A., 2016. Extension and inversion structures in the tethys–atlantic linkage zone, Algarve Basin, Portugal. Int. J. Earth Sci. 105, 1663–1679. https://doi.org/10.1007/s00531-015-1280-1.

Rey, J., Medialdea, T., 1989. Morfología y sedimentos recientes del margen continental de Andalucía Occidental. In: Díaz del Olmo, F., Rodríguez-Vidal, J. (Eds.), El Cuaternario de Andalucía Occidental, vol. 1. AEQUA Monografías, pp. 133–144.

Reynaud, J.Y., Tessier, B., Proust, J.N., Dalrymple, R., Bourillet, J.F., De Batist, M., Lericolais, G., Berné, S., Marsset, T., 1999. Architecture and sequence stratigraphy of a late Neogene incised valley at the shelf margin, southern Celtic Sea. J. Sediment. Res. 69, 351–364. https://doi.org/10.2110/jsr.69.351.

Rocha, J.S., Correia, F.N., 1995. Defence from floods and floodplain management in middle-size catchments. In: Gardiner, J., Starosolszky, Ö., Yevjevich, V. (Eds.), Defence from Floods and Floodplain Management, vol. 299. NATO ASI Ser, pp. 395–417. https://doi.org/10.1007/978-94-011-0401-2_25.

Rocha, F., Boski, T., Gomes, C., Moura, D., Veiga-Pires, C.C., 2004. Characterization of the sedimentary environment of the Gilão River mouth, based on sedimentological and mineralogical analysis. Thalassas 20 (2), 31–37.

Ronchi, L., Fontana, A., Correggiari, A., Asioli, A., 2018. Late Quaternary incised and infilled landforms in the shelf of the northern Adriatic Sea (Italy). Mar. Geol. 405, 47–67. https://doi.org/10.1016/j.margeo.2018.08.004.

Rosa, F., Rufino, M., Ferreira, Ó., Matias, A., Brito, A., Gaspar, M., 2013. The influence of coastal processes on inner shelf sediment distribution: the Eastern Algarve Shelf (Southern Portugal). Geol. Acta 11, 59–73. https://doi.org/10.1344/105.000001755.

Sousa, C., Boski, T., Gomes, A., Pereira, L., Lampreia, J., Oliveira, S., 2014. Holocene reconstruction of the Ria Formosa coastal lagoon (south of Portugal) based on a pre-Holocene paleosurface digital model. Comun. Geo. 101, 635–639.

Sousa, C., Boski, T., Pereira, L., 2019. Holocene evolution of a barrier island system, Ria Formosa, South Portugal. Holocene 29 (1), 64–76. https://doi.org/10.1177/0959683618804639.

Spanish National Geographic Institute, 2015. Mapa Topográfico Nacional 1:50.000 ráster de España, MTN50 ráster.

Stanford, J.D., Hemingway, R., Rohling, E.J., Challenor, P.G., Medina-Elizalde, M., Lester, A.J., 2011. Sea-level probability for the last deglaciation: a statistical analysis of far-field records. Global Planet. Change 79, 193–203. https://doi.org/10.1016/j.gloplacha.2010.11.002.

Stuiver, M., Reimer, P.J., Reimer, R.W., 2021. CALIB 8.2 [WWW program] at. http://calib.org. (Accessed 20 July 2021).

Telford, R.J., Heegaard, E., Birks, H.J.B., 2004. The intercept is a poor estimate of a calibrated radiocarbon age. Holocene 14, 296–298. https://doi.org/10.1191/0959683604hl707fa.

Terrinha, P., 1998. Structural Geology and Tectonic Evolution of the Algarve Basin, South Portugal. Imperial College London, p. 430. Ph.D. Thesis.

Tessier, B., 2012. Stratigraphy of tide-dominated estuaries. In: Davis Jr, R.A., Dalrymple, R.W. (Eds.), Principles of Tidal Sedimentology. Springer Netherlands, Dordrecht, pp. 109–128. https://doi.org/10.1007/978-94-007-0123-6_6.

Tesson, M., Labaune, C., Gensous, B., 2005. Small rivers contribution to the Quaternary evolution of a Mediterranean littoral system: the western gulf of Lion, France. Mar. Geol. 223–223, 299–311. https://doi.org/10.1016/j.margeo.2005.06.021.

Thanh, N.T., Liu, P.J., Dong, M.D., Nhon, D.H., Cuong, D.H., Dung, B.V., Phach, P. Van, Thanh, T.D., Hung, D.Q., Nga, N.T., 2018. Late Pleistocene-Holocene sequence stratigraphy of the subaqueous Red River delta and the adjacent shelf. Vietnam J. Earth Sci. 40, 271–287. https://doi.org/10.15625/0866-7187/40/3/12618.

Thomas, M.A., Anderson, J.B., 1994. Sea-level controls on the facies architecture of the Trinity/Sabine incised-valley system, Texas continental shelf. In: Dalrymple, R.W., Boyd, R., Zaitlin, B.A. (Eds.), Incised-valley Systems: Origin and Sedimentary Sequences, vol. 51. SEPM Spec. Pub, pp. 63–82. https://doi.org/10.2110/pec.94.12.0063.

Vail, P.R., 1987. Seismic stratigraphy interpretation using sequence stratigraphy; part 1, Seismic stratigraphy interpretation procedure. In: Bally, A.W. (Ed.), Atlas of Seismic Stratigraphy: AAPG Stud. Geol, vol. 27, pp. 1–10, 1.

Vanney, J.R., Mougenot, D., 1981. Memorias dos Serv. Geol. Port. 28, 86. https://doi.org/10.1007/BF02462809.

Vázquez, J.T., Fernández-Puga, M.C., Medialdea, T., Díaz del Rio, V., Fernández-Salas, L.M., Llave, E., Lobo, F.J., Lopes, F.C., Maldonado, A., Somoza, L., Palomino, D., 2010. Fracturación normal durante el Cuaternario Superior en la plataforma continental septentrional del Golfo de Cádiz (SO de Iberia). 1ª Reunión Ibérica Sobre Tectónica Activa y Paleosismología 179–182. https://doi.org/10.13140/2.1.1036.8009.

Veiga-Pires, C.C., Moura, D., Pedro, P., Correia, V., Duarte, D., Boski, T., 2000. Gilão and Almargem rivers evolution during late quaternary - preliminary results. INQUA Newsl 22, 79–80.

Vila-Concejo, A., Matias, A., Pacheco, A., Ferreira, Ó., Dias, J.A., 2006. Quantification of inlet-hazards in barrier island systems. An example from the Ria Formosa (Portugal). Continent. Shelf Res. 26, 1045–1060. https://doi.org/10.1016/j.csr.2005.12.014.

Van Geen, A., Adkins, J.F., Boyle, E.A., Nelson, C.H., Palanques, A., 1997. A 120 yr record of widespread contamination from mining of the Iberian pyrite belt. Geology 25, 291–294. https://doi.org/10.1130/0091-7613(1997)025<0291:AYROWC>2.3.CO;2.

Wang, R., Colombera, L., Mountney, N.P., 2019. Geological controls on the geometry of incised-valley fills: insights from a global dataset of Quaternary examples. Sedimentology 66, 2134–2168. https://doi.org/10.1111/sed.12596.

Wang, R., Colombera, L., Mountney, N.P., 2020. Quantitative analysis of the stratigraphic architecture of incised-valley fills: a global comparison of Quaternary systems. Earth Sci. Rev. 200, 102988 https://doi.org/10.1016/j.earscirev.2019.102988.

Weber, N., Chaumillon, E., Tesson, M., Garland, T., 2004a. Architecture and morphology of the outer segment of a mixed tide and wave-dominated incised valley, revealed by HR seismic reflection profiling: the paleo-Charente River, France. Mar. Geol. 207, 17–38. https://doi.org/10.1016/j.margeo.2004.04.001.

Weber, N., Chaumillon, E., Tesson, M., 2004b. Enregistrement de la dernière remontée du niveau marin dans l'architecture interne d'une vallée incisée: le Pertuis Breton (Charente-Maritime). C. R. Geosci. 336, 1273–1282. https://doi.org/10.1016/j.crte.2004.07.007.

Zaitlin, B.A., Dalrymple, R.W., Boyd, R., 1994. The stratigraphic organization of incised valley systems associated with relative sea-level change. In: Dalrymple, R.W., Boyd, R., Zaitlin, B.A. (Eds.), Incised-valley Systems: Origin and Sedimentary Sequences, vol. 51. SEPM Spec, pp. 45–60. https://doi.org/10.2110/pec.94.12.0045.